Modelling and Clustering of Climate Change Variables in Canada

A Thesis Submitted to the Committee on Graduate Studies

in Partial Fulfillment of the Requirements for the Degree of Master of

Science in the Faculty of Arts and Science

TRENT UNIVERSITY

Peterborough, Ontario, Canada

Applied Modeling and Quantitative Methods M.Sc. Graduate Program

January 2025

Abstract

Modeling and Clustering of Climate Change Variables in Canada

Alex Adenuga

Climate change is a global challenge with profound environmental, health, and socio-economic implications. Canada's diverse geography offers a unique lens to study localized climate trends. This thesis models and clusters climate variables, focusing on temperature trends, using Bayesian hierarchical models and clustering techniques to uncover regional patterns and health impacts.

Three decades of hourly temperature data from the Meteorological Service of Canada were split into 18 annual parts to capture seasonal variations. Metrics like mean, minimum, and extreme temperatures were analyzed. Bayesian models revealed regional variability, with examples of British Columbia and the Northern regions exhibiting notable trends.

Clustering identified regional dependencies and linked temperature trends with morbidity and mortality risks from air pollutants (PM2.5, O3). Summer risks stemmed from O3, while winter risks were PM2.5 driven. Findings highlight the need for region-specific strategies, offering actionable insights for policy makers addressing climate-health linkages.

Keywords: Climate change, Bayesian models, clustering, temperature trends.

Acknowledgements

I would like to express my deepest gratitude to my exceptional supervisor, Dr. Wesley Burr, whose unwavering support and guidance have been instrumental to my academic success at Trent University. From my very first day to the completion of this program, Dr. Burr has been a mentor, counsellor, and teacher both academically and personally. His dedication and encouragement have made a profound impact on my journey, and for that, I am truly grateful.

I would also like to extend my heartfelt thanks to Dr. Hwashin Hyun Shin and Health Canada for their invaluable contributions to this work. Their inspiration, the detailed data provided, and partial funding made this research possible.

To my incredible wife and little one, thank you for your patience and understanding. Despite the countless hours I spent at my computer working on this thesis, your love and support remained my source of strength (even with occasional interruptions). I love you both deeply.

Finally, to my family members, friends, and everyone who supported me through this journey, thank you from the bottom of my heart. Your encouragement and belief in me made all the difference.

Table of Contents

List of Figures

List of Tables

1. *Introduction*

Climate change is one of the most pressing global challenges, with profound impacts on environmental systems, human health, and socio-economic structures. In Canada, the effects of climate change are especially significant due to the country's diverse and sensitive ecosystems. Understanding the variability in climate change indicators, such as temperature, precipitation, and other atmospheric conditions, is critical for developing adaptive strategies to mitigate the adverse effects. Traditional statistical methods have provided valuable insights into climate change patterns, but the complexity and uncertainty inherent in these variables call for more advanced approaches. Bayesian modeling, with its ability to incorporate prior information and account for uncertainty in predictions, offers a powerful framework for analyzing climate change data, making it a crucial tool for policymakers and researchers alike. Clustering of climate variables is an innovative way of visualizing correlations between different groups irrespective of geographic characteristics to understand better climate dependencies and independence in the pattern of climate change dynamics and variability that is equally useful for Canadian policymakers for implementation of policies that can either be local, regional or national.

This research focuses on applying Bayesian modeling and clustering techniques to climate change variables in Canada. By leveraging Bayesian methods, this research aims to enhance the understanding and modeling of climate change using an unconventional model technique and to identify clusters of similar climate patterns across

different regions. These clusters can identify regions with similar climate behaviours, such as climate variability and concentrations of air shed pollutants, and also identify clusters of morbidity and mortality risks related to the deposits of these air shed pollutants, enabling targeted mitigation and adaptation measures. This approach supports efforts to reduce hazardous health impacts, which can lower the risks of hospitalizations and mortality. The integration of Bayesian inference allows for more flexible modeling of complex climate variables while addressing the uncertainty and variability inherent in the data, ultimately contributing to a deeper understanding of climate change dynamics in relation to air pollution across different regions in Canada.

This work involved the use of hourly temperature data from the Meteorological Service of Canada climate database that had been previously processed and cleaned into SQL format by researchers working on a Health Canada grant. We start by discussing previous research around climate change and researchers' methods from around the world and Canada to understand how climate change research had been done before now, discussed in Chapter 2. We then proceeded to discuss and build an analytical pipeline, which involved the splitting hourly data into annual slices before constructing models for trends over long timescales. These trends were combined in a Bayesian modeling framework, allowing regional analysis of climate variability in Canada, with the results detailed in Chapter 3. In Chapter 4, we performed clustering analysis, exploring regional intricacies and dependencies, and then looked at areas with regional deposits of air shed pollutant with observed climate change occurrences in view to observing the risk to inhabitants of these regions. Finally, we clustered the morbidity and mortality risks due to the ambient air pollution exposure, and concluded with a comprehensive discussion of all the analyses that were performed and some future work to consider.

2. *A History of the Study of Climate Change*

While weather, climatic variations, and extreme events have been observed and documented since classical times, it was not until the 19th century that meteorological instrument networks were established on a national level all over the world [8, 10]. Some of the classical eras where documentation of climate as a function of latitude were described by Greek astronomer-geographers like Erastosphenes (3rd century BCE) and Ptolemy (2nd century CE) [50]. One of the first climate research projects that described climate beyond the concept of latitude was in 1686 by Edmond Halley, who sought to understand the physics of the trade winds [18]. Halley published the theory that solar heating caused air to rise near the equator, such that the rarefied air caused denser air from higher latitudes to 'rush in', creating the trade winds [24]. After Halley, the atmosphere's greenhouse effect was pointed out by Fourier in 1827 [21], who suggested that human activity can modify the climate. There were several other documentations about weather research, and climate variability that have allowed insights into climate variations on a daily to decadal scale; see Bronnimann *et al.* who provide a detailed inventory of metadata on globally available early instrumental data before 1850CE [10, 9].

The formal foundation for the greenhouse theory of climate change was laid in 1896 by Arrhenius [2] who dealt with the climatic effects of changes in atmospheric CO_2

and how water vapour contributes to Earth's surface temperature. His 1896 paper calculated that doubling atmospheric CO_2 would raise the global average temperature by $5 - 6°C$ [77, 65, 18].

2.1 Climate Change is not just Temperature

Temperature data is one of many data collected as Earth Observation (EO) type data. These EO data are collected to provide evidence on the past, present, and future of the state of the Earth. It is important to know that an international and multi-agency group covering different climate domains (Atmosphere, Oceans, and Terrestrial Systems), established in 1992 and endorsed by the United Nations called the Global Climate Observing System (GCOS) is responsible for making sure that these EOs are available, accessible, preserved, sustained, coordinated, and improved. The GCOS is also responsible for identifying principal observations to be addressed by a set of space missions and other EO networks to characterise the state of the global climate system and to support the monitoring and planning of mitigation and adaptation measures [20]. These observations are called Essential Climate Variables (ECVs) [69, 5].

2.1.1 Essential Climate Variables (ECV)

Following the Global Climate Observing System (GCOS), Essential Climate Variables (ECVs) are physical, chemical, or biological variables or groups of linked variables that play a crucial role in characterizing Earth's climate [69] [57]. The GCOS currently identifies 54 ECVs, categorized into three main domains: Atmosphere, Land, and Ocean. The Atmosphere domain is further subdivided into Surface, Upper-air, and Atmospheric Composition. The Surface category includes ECVs such as Temperature, Precipitation, Pressure, Radiation budget, Water vapour, and Wind speed

and direction. The Upper-air category comprises ECVs like Earth radiation budget, Lightning, Temperature, Water vapour, Wind speed and direction, and Clouds. Atmospheric Composition includes ECVs such as Aerosols, Carbon dioxide, methane and other greenhouse gases, Ozone, and Precursors for aerosols and Ozone. For a comprehensive list of ECVs under the Land and Ocean categories, please refer to [69].

A number of research projects have been done on one or more of the ECVs to evaluate the variability and complexity of climate change over the years. A paper published by Xiaoyan and Zong-Liang [34] titled *Projected Changes of Temperature and Precipitation in Texas from Downscaled Global Climate Models* explored the future change in temperature and precipitation in Texas based on the averages from 1971 to 2000. They applied a statistical downscaling technique, a bias correction approach introduced by Wood *et al.* [86] and modified by Maurer [51]. The goal of the downscaling approach was to downscale the climate projections of General Circulation Models to regional scales. This same method was used by Jaime *et al.* [29] to model climate change scenarios for temperature and precipitation in Aragon (Spain), and by others: [30] for Sweden; [67] for the European Alps, [28] for the United Kingdom; [62] for California and so on.

Ziwen *et al.* [88] in 2022 extended this research for the Northeast United States by adding another ECV called hourly Pressure Change Event (PCE) to the mix. They used stochastic downscaling by using a multivariable Markov Chain on the Global Circulation Models instead of the simple statistical downscaling previously used, to detect the variability and form projections for regional climate change.

Notable among research investigations into the interplay between climate change and ozone depletion attributable to air pollution is the study conducted by Collette *et al.* [3]. In the paper titled *European Atmosphere in 2050, a Regional Air Quality and Climate Perspective under CMIP5 Scenario*, they aimed to quantify the impacts

of climate change and global pollution on ozone and particulate pollution in Europe, assessing the associated benefits and penalties. Similar to the methodologies used by others [88, 34, 86], they used the downscaling of the Global Circulation Model to regional scale from the Large-scale atmosphere-ocean General Circulation and Global Chemistry Transport Models. The study covered a 10-year simulation to be able to gain statistical significance and minimize the effect of interannual climate variability. The data used was daily maximum time series data from 1998 to 2007 for Ozone and daily mean of PM_{10} from the database of the European Environmental Agency. Previous research that used the same model established that the model exhibits a cold bias of sea surface temperature over the North Atlantic due to a strong underestimation of the Atlantic meridional overturning circulation [31]. This study found that the difference in summertime temperature and incoming short-wave radiation can also modify the biogenic emissions of ozone precursors [3].

2.2 Climate Models and Computation

Widespread instrumental records of hemispherical scale surface temperature only began after the 1850s [65]. Going back in time, information on climate with annual or seasonal resolution were deduced from either natural proxies, such as tree rings, ice cores, corals, and sediments, or documentary evidence from the archives of societies [10]. The Vienna Meteorological Congress of 1873 acted as a catalyst for many countries to establish their own meteorological agencies [32]. Even though the advent of instrumental measurement was a progressive one and enabled several possibilities in terms of climate research and its computation, it came with considerable discrepancy in even the signs of the changes in climate between the 1850s and 1900 which is largely due to inadequacies in available data [39, 19, 59, 65, 38, 44, 29].

However, there were dynamically consistent estimates of the atmospheric state

from 1851 to 2008 from global coverage of the 3D atmosphere from historical reanalyses that assimilate surface and sea level pressure and in some products like marine winds [13, 45, 29, 63]. In addition, the advent of a new generation of meteorological instruments placed on satellite platforms in the 1960s, and their continued development into the 1990s has now given the potential for actual global estimates to be made of a much wider variety of climatic variables than previously [32].

When it came to computing climate change issues through precipitation, the primary resource is two of the longest regional precipitation series for the subtropics; they were those representative of the Indian subcontinent from 1871 and of South Africa from the late 1880s [32]. Work in the latter region has been performed largely by Tyson [76, 32] who observed a quasi-regular 18-year oscillation in annual precipitation with dry phases around 1913, 1932, 1950, 1970, and 1986.

When it comes to assessing climate change in terms of temperature, the longest and most detailed examination of the global mean surface temperature based on instrumental records has been the one performed by Jones *et al.* in 1986 [39, 35, 36, 37]. This time series of monthly hemispheric and global mean temperature started from around 1854 and combined data from approximately 2000 land-based stations along with millions of ship observations of marine air temperature and sea surface temperature until the year 2000 [7, 32]. Usually, the methods used in these publications were multiple regression after adjusting for possible sources of biases like urban warming bias [40] and/or changes in measurement procedure for temperature observations on board ships [35]. The study showed that the planet has warmed at the surface by 0.45 ± 0.15°C since the middle of the 19^{th} through the 20^{th} century. In these works Jones noted that the warming has not been continuous through time and space, since there was rapid global warming from the 1910s to 1940s and again from the 1970s to 2000. He also noted that there were fairly constant and declining temperatures in the periods 1860 - 1900 and 1940 - 1970, respectively.

Further to success in instrumental measurements in temperature, in the late 1980s research on statistically making inferences about climate variability was published by Richard W. Kartz [85]. The main goal of this research was to describe a statistical procedure for making inference in scale that would be appropriate when it comes to dealing with time series of historical climate data. The statistical methodology he proposed was the estimation of innovation variance and then making an inference about the innovation variance by estimating the parameters of an autoregressive model; the estimates of the parameters served as the magnitude of change in variability in climate based on the specific station locations of the data.

In research published about temperature in the 21st century by Turko *et al.* [75], the authors used temperature and precipitation to observe climate change hotspots. Similarly, there have been several studies like [26, 27, 41, 54] who jointly explored the effects of climate change using variations in temperature means that are examined on a global scale. In their research, a method that had been used by [14] was used to capture the climate change hotspots: the method involved aggregating changes in the mean and variability of seasonal temperature and then including information on seasons that exceeds the baseline extremes. Furthermore, in 2018 Simon *et al.* [60] explored the Highest Temperature of the Year (HTY) for Global, Regional, and Megacity, using daily maximum temperature records from the Global Historical Climatology Network from 1966 to 2015 and 1986 to 2015. In the study, the statistical significance of the observed trend was determined by calculating the exceedance probability of the observed slope based on Monte Carlo simulation of 5000 samples from an autoregressive (AR1) model. The study showed that all available cells in the northernmost territory of Canada, Nunavut, have positive trends, with some showing increasing rates of more than 0.60°C per decade.

A very recent study reported by the National Oceanic and Atmospheric Administration (NOAA) Annual Climate report for 2023 affirmed that the combined land

and atmospheric temperature has increased at an average rate of 0.11° Fahrenheit (0.06° Celsius) per decade since 1850, or about 2°F in total. And further, that the rate of warming since 1982 is more than 3 times as fast: 0.36°F (0.20°C) per decade [58].

2.3 Climate Change Research in Canada

Canada's diverse geography encompasses a wide range of climates, landscapes, communities, and economic profiles, both between and within its various regions, making it a country of remarkable complexity and variability. Hence, climate researchers in Canada have been profoundly interested in how Canada is mitigating and managing climate change for a long time. Hence, there has been some Canada-centric research that has been majorly influenced by anthropogenic climate change. In 1986 Wright *et al.* [15] published a preliminary report on oceanic changes associated with global increases in atmospheric carbon dioxide under the Canadian Technical Report of Fisheries and Aquatic Sciences. They suggested that with a doubled CO_2 climate, there may be general warming and freshening of the continental shelf waters in eastern Canada. The study aimed to examine possible changes in the marine environment that might influence the Atlantic Canadian fisheries industry. They used the General Circulation Models to speculate on possible oceanic changes, particularly in the North Atlantic Ocean. They determined that climatic changes due to increased atmospheric CO_2 had not yet been conclusively observed. Based on their model, they suggested that the water off eastern Canada would have warmer ocean temperatures, reduced surface salinities, and increased along-shelf residual currents associated with a stronger Labrador current. However, they noted that it is impossible to give reliable quantitative predictions as more development was needed in remedying the unrealistic nature of atmosphere-ocean-cryosphere in the General Circulation Model.

After Wright *et al.* highlighted some of the inadequacies with the Global Circulation Models, in 1990 Mysak and Lin [55] published a review of some of the regional and global research related to climate change and oceans that had been published before 1990. In this work they noted that the study of Canadian climate through oceans and Arctic sea is crucial due to the significant impact of sea ice formation on the atmosphere. When sea ice forms, latent heat is released into the atmosphere, and the ice then acts as a barrier, hindering heat exchange between the atmosphere and the relatively warm ocean beneath. Since the Earth's reflectivity (albedo) varies with the extent of sea ice, understanding the dynamics of Arctic sea ice variability is essential for grasping the complexities of the Canadian climate. They noted in their concluding remark that it is difficult to distinguish greenhouse warming from natural climatic fluctuations. They also wrote that there is a need to learn more about the complex physical, chemical, and biological interactions among different components of the climate systems. Furthermore, they suggested that these research improvements could be achieved through collecting and analyzing environmental data and developing more accurate mathematical models of the climate systems. However, it has been observed that many researchers used the regional Global Circulation Models which focused on changes in long-term average (i.e., annual, seasonal) temperature [6] for Canada in the 20^{th} century.

In 2001, Bonsal *et al.* [6] noted that in describing the spatial and temporal characteristics of daily and extreme temperatures accurately, long-period time series of reliable and homogeneous daily values are required. They and Vincent *et al.* [80] stated that such data had been recently created for Canada and was used in the paper *Characteristics of Daily and Extreme Temperatures Over Canada*; details of the cleaning and preparation of these data sets can be found in [79, 80, 82]. The main goal of the research paper was to use the data to examine the 20^{th} century trends and variability in daily temperature characteristics, with specific emphasis on

the extreme ends of the daily temperature distribution over Canada. The researchers employed temperature percentile trend analysis to assess climate variability in the 20^{th} century, utilizing temperature data to examine trends and patterns in the climate system. They uncovered significant spatial, temporal, and seasonal variations in temperature trends across Canada, with the largest magnitude and most important changes occurring in western regions during winter and spring. Notably, southern Canada experienced a marked decrease in extremely cold days during winter, spring, and summer between 1900 and 1998, as indicated by both low and high percentiles of daily minimum and maximum temperatures. While a slight increase in extreme heat days was observed during winter and spring, this trend was far less pronounced than the decline in extreme cold days. Regional differences were most apparent during winter and spring, consistent with the findings of [89]: that Canada is experiencing a decrease in extreme cold temperatures, rather than a uniform warming trend.

Several studies and estimates of climate variability in the 21^{st} century in Canada have been done by researchers through time series temperature and precipitation trend analysis. Some of these studies include Bonsal *et al.* [6], Turner and Gyakum [33], Vincent *et al.* [79, 80, 82, 83, 81] and Zhang *et al.* [89]. Specifically, Vincent *et al.*, Bonsal *et al.* and Zhang *et al.* evaluated the shifts in the distribution of daily temperatures across Canada; they analyzed temperature percentile trends. Specifically, the 5th, 10th, 25th, 50th, 75th, 90th, 95th, and 99th percentiles of both daily minimum and daily maximum temperature distributions were calculated, providing insights into changes in temperature extremes and variability. Turner and Gyakum modified the methodology by using 30-year running mean climatology centred around a specific period used for trend calculation and then applied a 15-day smoother. The results from these studies showed that Canada is not entirely getting warmer, but that cold temperatures are getting rarer in Canada.

In a comparison of Canada's temperature to the United States, Karl *et al.* [40]

wrote that an appreciable number of non-urban stations in the United States and Canada have been identified with statistically significant (at the 90 percent level) decreasing trends in the monthly mean diurnal temperature range between 1941 to 1980. The proportion of stations in the network exhibiting a decrease is significantly higher than would be expected by chance alone, with a peak occurrence in late summer and early fall, and the smallest in December [78].

2.4 Conclusion

A wealth of research has been done on the study of climate, and on climate change specifically, including some directly focused on the Canadian experience. We will take inspiration from these previous works, and the approaches considered, in our development of localized climate variable trend models in the following chapters.

3. *Modeling for Localized Climate Change Detection*

This chapter discusses the data preparation and computational methods involved in modeling and detecting climate variability in over 3 decades of time series temperature data. The goal of this development is localized trends in climate that can then be pooled or clustered for exposure of commonalities across Canadian sub-regions, for possible eventual use in climate and air pollution risk models for health. We thank Health Canada for the inspiration behind this work, and both the Meteorological Service of Canada and Environment and Climate Change Canada for their stewardship and hosting of the requisite data sets.

3.1 Temperature Data

Temperature and other climate variables data were extracted from the Meteorological Service of Canada climate database. The database formed contains hourly temperature and other climate variables data from climate stations throughout Canada. Monthly `.csv` files initially organized the data for each climate station but were then processed and stored. The data were stored in SQLite, a flatfile database engine accessed from within R using the `RSQLite` package [56]. The data used for this study was then directly extracted from the database. Shown below is a table describing the

regions and the number of climate stations in the database with varying years of data availability. The period of interest for this study is from 1989 to 2018:

Region	**Number of Climate Stations**
Region 1 (British Columbia)	1771
Region 2 (Northern Region)	565
Region 3 (Prairies)	2781
Region 4 (Ontario)	1642
Region 5 (Quebec)	1096
Region 6 (Atlantic)	942
Total	**8797**

Table 3.1: Number of Climate Stations by Region

The pipelines and steps followed to process the temperature data are further explained below:

3.1.1 Time Series Data Split

It is challenging to make accurate predictions of overall trends due to a number of non-stationarities in real-world climate times series data [47]. Hence, analyzing the entire time series at a time overlooks this distribution discrepancy and would assume that all time points within the same instance share the same statistical properties. However, splitting a huge time series into smaller, equal parts may reduce the time dependencies and distribution discrepancies inherent over time, fostering better prediction accuracy. This is the philosophy we implement in the following.

The method began by splitting the time series data across each year of available data into 18 separate sections. We decided to split the entire time series into smaller parts to assess the variability embedded in these small parts. It is worth noting that

the decision to split into specifically *18* parts is not due to existing literature, but was chosen specifically to both be able to access the variability in smaller periods, while also allowing for smooth transitions through the leap year. This results in segments that are 487 hours long, which across 4 full calendar years (including one leap year) will synchronize and repeat. As the source data we considered was hourly, this effectively determined the constraints on our choice, and led to this choice of 18. As we will see in the following, there appear to be no significant impacts of this choice versus other, similar choices. In Figure 3.1, we demonstrate a graphical representation of the split of a specific station. This split is eventually performed on all the stations considered.

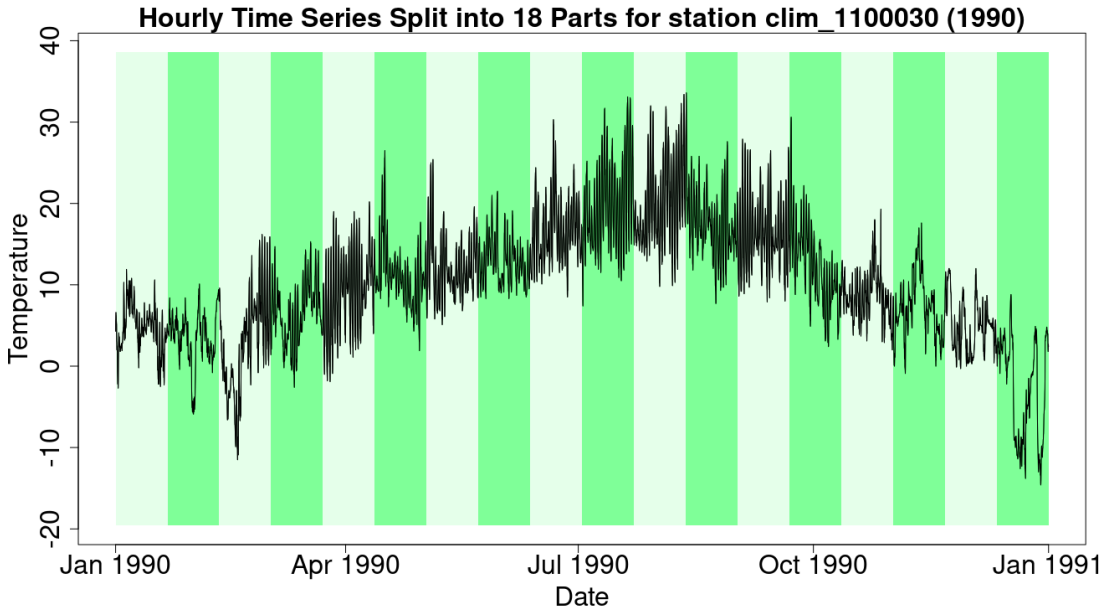

Figure 3.1: Plot showing the split of hourly temperature for station `clim1100030` for 1990 into 18 equal parts, denoted by the light and deep green vertical bar colours.

Figure 3.1 shows that the temperature for this station was as typical of Canada's temperature, which is usually low at the beginning of the year, higher in the middle of the year (summer), and low again at the end of the year. Upon splitting the data,

we see the periods and data that fall within a specific bar for of each of the 18 parts (visualized as either light green or the deep green) are what we will put together to continue the analytical pipeline in this study.

3.1.2 Computing Metrics for the Splits

After splitting the time series data into 18 rolling parts, the next step is to compute a summary metric (or several metrics) for each element of the split. The idea is to compute any desired metric for each group of the collected splits for each year, where the group could be "all of the first elements in a year", for example. For instance, we might compute mean, maximum, minimum, 90^{th} percentile, etc., examples of which are shown in Figure 3.2.

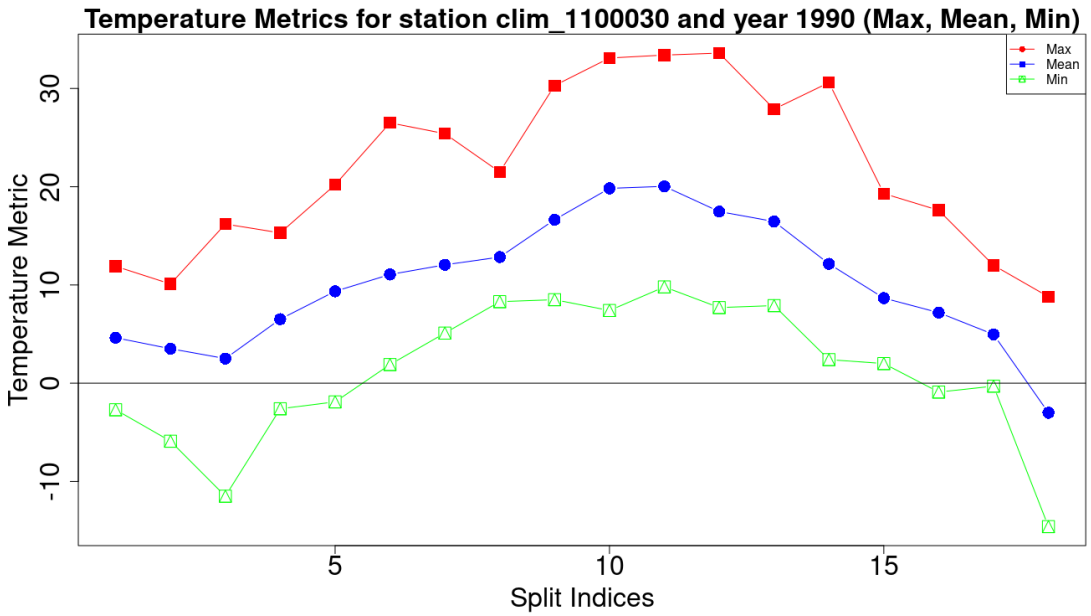

Figure 3.2: Plot of computed Mean, Maximum, and Minimum for station `clim1100030` for the year 1990.

Looking at Figure 3.2, we can observe that the shape of the mean plot mirrors the shape of Figure 3.1 because each point is a group average of the observations

plotted in Figure 3.1. In addition, the minimum, maximum, and mean showed quite similar behavior regarding the seasons of reducing and increasing trends with no visible erratic behaviour for this station in 1990.

3.1.3 Modeling the Computed Metric

Now we arrive at the point of doing these splits. We can then take split elements *over time*: the set of every 19^{th} element in chronological order is inherently annual in nature, and will correspond to the same "time of year", without being biased by the leap-year calendar, or strangely weighted by using the calendar months. When we are considering very subtle trends over time, we want to protect ourselves from these biases, which is the impetus behind the perhaps strange-seeming choice of 18 segments per year.

Then after computing the desired metric for each element of each year, we perform regression analysis: the choice of regression model (simple or robust) depends on the level of complexity desired in the model. In our case, as a proof-of-concept, we performed simple linear regression on the sets of indexed elements across years. However, to be able to perform the simple linear regression, we had to clean and filter the data to ensure we had enough data points within the desired study period (1989 to 2018) for the stations to be included in the regression analysis. Hence, we added the condition that the linear regression should only be performed if we have at least 10 years of data points for each of the split indices in view of minimizing regression standard error. Shown below is a table of the number of climate stations with sufficient data by region (Table 3.2) and the results of the linear regression being visualized in Figure 3.3

Region	Number of Climate Stations
Region 1 (British Columbia)	10
Region 2 (Northern Region)	4
Region 3 (Prairies)	7
Region 4 (Ontario)	13
Region 5 (Quebec)	22
Region 6 (Atlantic)	5
Total	**61**

Table 3.2: Number of Climate Stations by Region with sufficient data

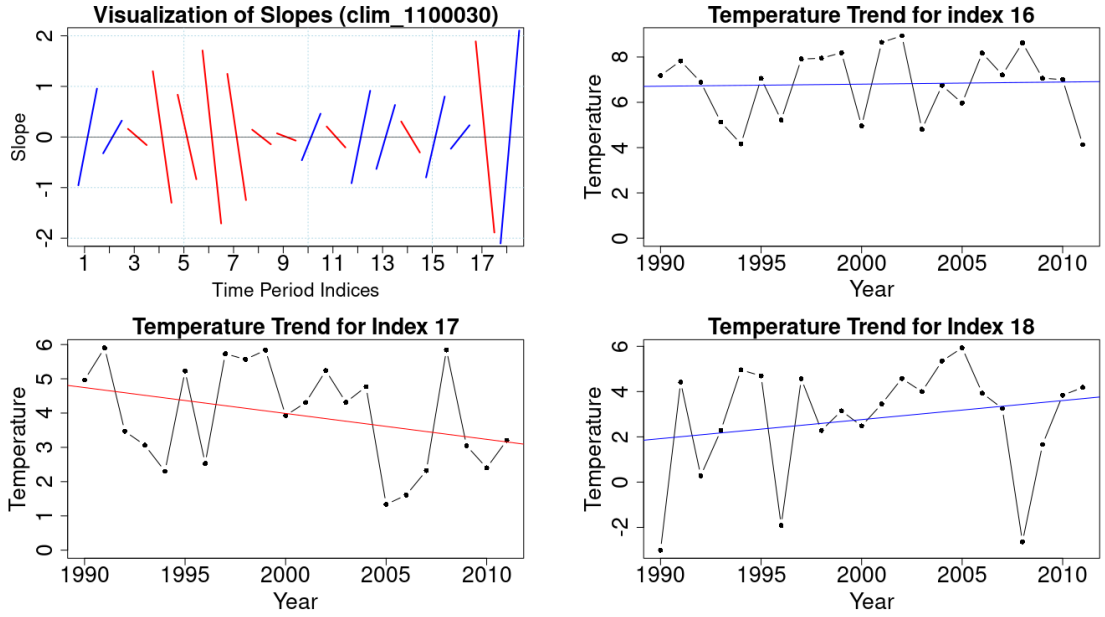

Figure 3.3: Plot showing four facets: (a, top left) the slopes for metric "average hourly temperature" from Indices 1 to 18 across 30 years of data, by index; (b, top right) estimated slope for index 16; (c, bottom left) estimated slope for index 17; and (d, bottom right) estimated slope for index 18. These indices were chosen somewhat arbitrarily to demonstrate the method.

The first plot on the top left of Figure 3.3 shows the difference in the magnitude

of the slopes from index 1 to 18. How long the line is indicates how large the slope of the model is. The red colour signifies a negative slope, while the blue indicates a positive slope. Looking at how long the lines are, we see that the largest change over time occurred around the 18th index while the smallest appears to have occurred on the 9th index. In general, we had positive slopes in the first 2 periods, then a consistent negative slope until the 9th index, before the intermittent change in these slopes between positive and negative. These changing values in slope across this 30-year set of hourly data demonstrates the erratic changes in climate in the exhibited station, how swiftly the temperature and season have been changing in the study period for this station, and suggests that there may be adjustments to the seasonal boundaries for this station. This last may be indicated by the transitions from warming to cooling trends, and from cooling to erratic (alternating) trends, and will be a point of discussion in the coming work.

The other 3 faceted plots in Figure 3.3 are excerpts from the first plot for indices 16 to 18, and show the line of best fit for the slopes in each of these indices, displaying the red line for decreasing slope and the blue line for increasing slope and specifically showing the extent of reduction or increase. These figures hopefully make clear how the pooling occurs: first, across the 487 hourly samples via the metric (hourly mean); then across 30 years of data via regression (facets b, c and d); then aggregated by time period index to give localized trends by time element for a given station.

Figure 3.3 demonstrates a similar result to the research performed by David M. Romps [66] recently. In this work, Romps observed that heat index extremes are increasing several times faster than air temperature – this is evident in the index 16, 17, and 18. As these plots are of the hourly averages, unweighted, extremes should drive the averages up (or down) for a given $\approx$20 day time period element. And we do see some rapid changes year-to-year, e.g., 2008 in index 18 is exceptionally low, while it is quite high in index 17. So this indicates warmer than average weather in

late November, early December in 2008, followed by significantly colder weather than average in December proper through to the New Year. This matches the findings of Romps.

Now, our interest is in Canada as a whole. One station means essentially nothing in that grand scheme, and we cannot use it to generalize on the climate variability or change in Canada. Instead, we have to apply these steps to a number of stations across Canada to then have enough information to pool the results, and compute the regional or national trends. The conventional way to pool such information is to use Bayesian hierarchical models, which we describe in the following.

3.2 Bayesian Hierarchical Modeling

Bayesian Hierarchical modeling is a framework for integrating numerous data sources and statistical modeling results into a single statistical model [48]. Bayesian hierarchical approaches allow for combining data from multiple groups, acknowledging that each group may have its unique characteristics, rather than assuming they all share a common population distribution [17]. There are two advantages as stated by Dunson [16] on why we might want to apply the Bayesian approach: the first is that using an informative prior distribution utilizes existing knowledge of the parameter values obtained from the historical context discussed in Section 3.1.3; and the second is that the posterior probabilities are applied after that. We update this declared prior distribution by selecting a prior probability distribution for unknowns in the model and then use Bayes' theorem to produce a posterior distribution. By doing this on the localized estimates of trends, we can pool the information regionally or nationally in order to compute regional and national variations in temperature. This technique has been used on temperature data in a number of previous works [73, 72, 74, 68, 42, 4].

3.2.1 National Temperature Change Estimate

We will attempt the use of a Bayesian hierarchical framework to estimate the national temperature change in Canada by first estimating the posterior without covariates, and then with regional covariates. It is worthy of note that the posterior distribution is computed through the feeding or pooling together of parameters in the model, and it is the objective of most analysis like this one.

3.2.1.1 Single Level Model with no Covariates

The simplest model for this is the single-level model, which involves only the station-level estimates of slopes. We then assume that each of these (by index, say) has been drawn from a common, shared distribution. One instantiation of the model is defined as:

$$\mu \sim \mathcal{N}(0, 5)$$

$$\sigma \sim \text{Cauchy}(0, 2)$$

$$\beta_c \sim \mathcal{N}(\mu, \sigma)$$

$$\hat{\beta}_c \sim \mathcal{N}(\beta_c, Se_c) fbgf$$

where the $\hat{\beta}_c$ elements are the station-specific mean temperature trends. Note that the `Cauchy` referenced here is in Stan notation, and is actually a *log-Cauchy* distribution, as recommended by Gelman *et al.* [71]. These station-level means are assumed to be drawn from a common national distribution with hyperparameters μ and σ. These parameters are given weakly informative priors to incorporate some assumptions about the likely scale of μ and σ, butare still broad enough to allow the data to have significant influence.

3.2.1.2 Two Level Regional Model with Covariates

The two-level models adds a layer to the hierarchy under the assumption that the average temperature trends are regionally influenced. It emphasizes a regional influence between stations, and assumes that the specific geographic region of the station shares a common distribution. Hence, the second-level national distribution is assumed to be the source of the regional distribution. Just like the single-level model, it was designed with weakly informative priors as shown below:

$$\sigma_c \sim Cauchy(0, 2)$$

$$\sigma_r \sim Cauchy(0, 2)$$

$$\mu \sim \mathcal{N}(0, 5)$$

$$\mu_r \sim \mathcal{N}(\mu, \sigma_c)$$

$$\beta_{c,r} \sim \mathcal{N}(\mu_r, \sigma_r)$$

$$\hat{\beta}_c \sim \mathcal{N}(\beta_{c,r}, \mathrm{SE}_c)$$

where σ_c represents station-level variation while σ_r stands for the between city variations within the region. In this model representation, it is assumed that $\hat{\beta}_c$ have been drawn from a common station-specific distribution that is within a specific regional distribution which is centred on μ_r and has a standard deviation of σ_r. In concluding the computation, μ, the average temperature trend, is the centre of the national distribution. So the set of μ_r are drawn from the common national distribution with centre μ, and then each station's underlying mean trend is drawn from its respective regionally centred distribution, giving $\beta_{c,r}$. Our estimation goal is the highest level of the hierarchy and the mean, μ.

The graphical presentations of the results of the model are presented in the following section.

3.3 Results and Discussions

The figures below explain the extent of temperature trend variability and thus emphasize the rate at which the climate has changed for the entire period considered. In particular, they show the importance of change in each split indices from 1 to 18. The model specification is a standard 4 chains mixing with 100,000 replications [23] where the first 2,000 were specified to be the warm-up. The slopes and standard error from the initial regression performed, and subsequently used as the input into the Bayesian model, were each multiplied by 1000 to enable conspicuous visualizations of the results (mainly by taking the figures away from the origin since the values for the slope were very small).

3.3.1 Single Level Model

Model Diagnostics

In Bayesian modeling, when the different chains have converged to the posterior, they should "mix" well. The extent to which the chains are mixing can be quantified by the "R-hat" statistic [23] which compares the within-chain variance to the between-chain variance; for chains that mix well the R-hat statistic is close to 1. An R-hat statistic larger than 1.1 is considered problematic [22, 61]. The model diagnostics showing Rhat values for comparison to this 1.1 cutoff are included in this thesis as Table A.1 in the Appendix.

1-Level Model Posterior Density

As a starting point, consider pooling every single index together: so, all trends, all indices, all drawn from one common national distribution. In this case, we get something like Figure 3.4.

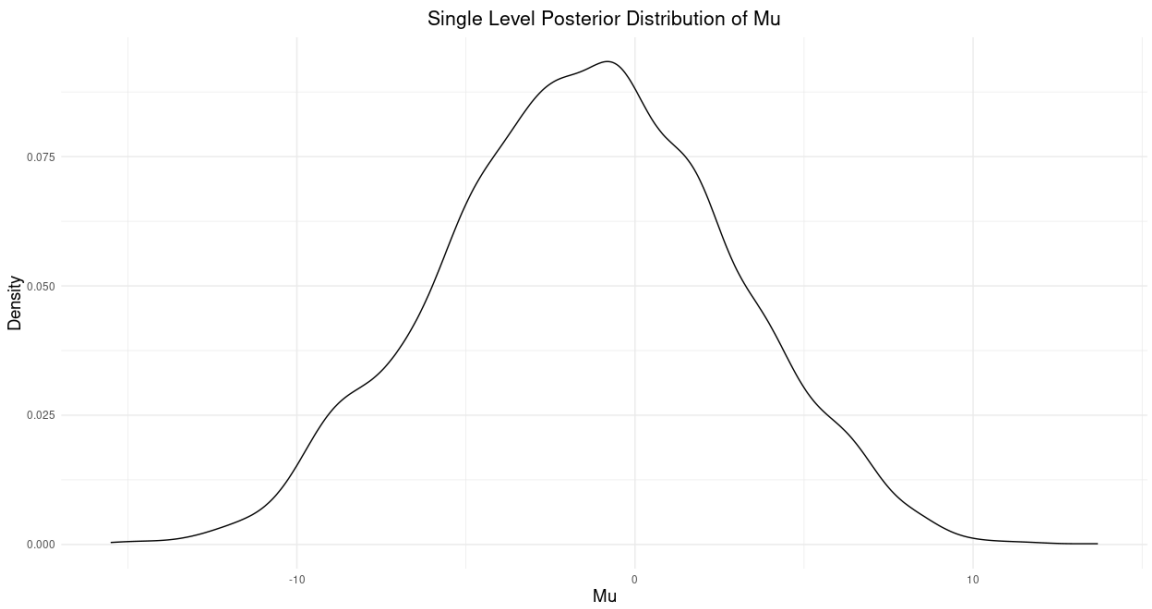

Figure 3.4: Posterior Density for the Single Level Model for Average Temperature National Mean Trend (μ).

This posterior density for the average temperature trend μ for the single-level model appears to be approximately normally distributed with one mode. The distribution is not smooth, however, and the minor blips in the distribution may be indicative of some multimodal behaviour in the data coming through in the posterior. In particular, this may indicate that the indices are clustering around individual modes (as one would expect), or that there are regional differences.

Average Temperature Change at each Split Index

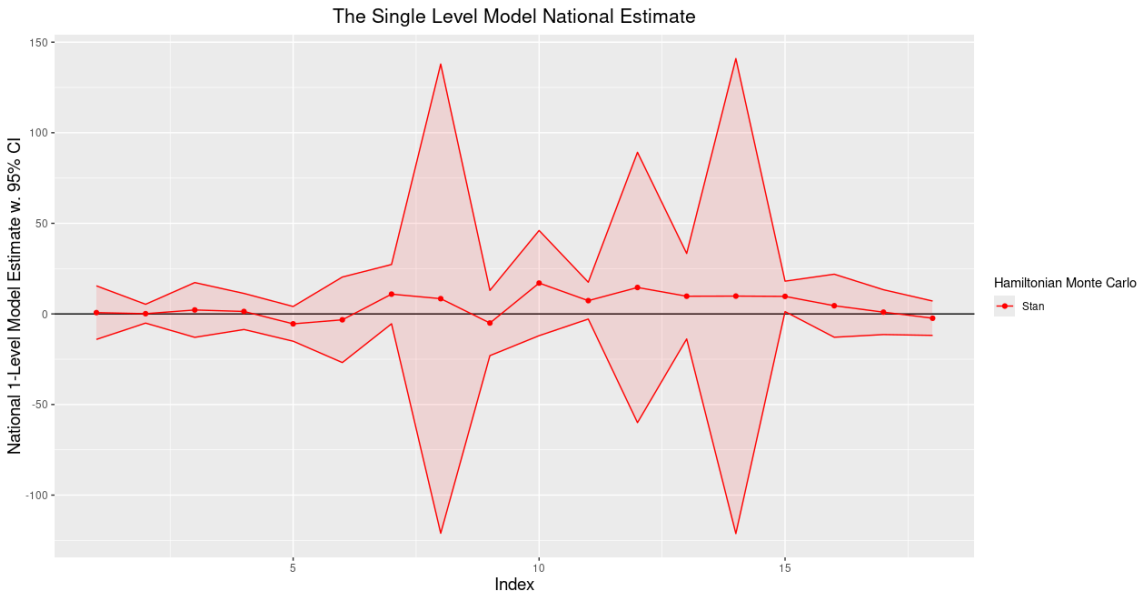

Figure 3.5: Single-Level Posterior Mean Trend with variation for each index, 1-18.

Figure 3.5 shows the rate of change in the average temperature across the split indices with their respective pointwise 95% credible intervals. Looking at the plot, the rate of change in temperature is approximately at the same level from the indices 1 to 6 (and quite small). However, the credible interval from indices 7 to 9 and 12 to 15 are very large, suggesting poorer model fits or structural problems. The most important peak seen in the plot is the change from indices 9-10 as there appears to be a dip of less than zero in a time that is supposed to be a warm season of the year (summer). Specifically, the national trend at index 7 and 8 are positive, 9 is negative, then 10 is quite positive (in fact, the most positive of all indices). So warming, warming, colder than expected, exceptionally warming.

Generally speaking, Figure 3.4 indicates that the national estimated mean temperature trend is -2.4, which in reality is -0.0024 (recall: the original data was multiplied by 1000 to be able to visualize the numbers away from the origin). This is the mean

trend in these localized, indexed temperatures in Canada from 1989 to 2018. The fact that the value is negative does *not* suggest that the overall trend of average temperature in Canada is 0, however, simply that if we naively pool the different trends-of-means, we get an overall negative effect. Because we are examining small periods of time as the elements of the trend, shifting seasons can easily result in large numbers of negative trends. This becomes more clear when we examine the individual indexed trends in Figure 3.5. There, 5 of the 18 indices have negative mean trends, while 13 are positive. However, many indices are nearly 0. Functionally, Figure 3.5 indicates that coarsely pooling all the trends is not a useful thing to do. In the next section, we consider pooling regionally as well as by index.

3.3.2 Two Level Model

Recall from above that this model added a regional hierarchy to the mix, in which the model assumes that the within-station and between-region variations follow the structure provided. We apply this model to the same data as above.

Model Diagnostics

The figure below is a trace plot for the 2-level model. The results of other diagnostics are in Table A.2 in the Appendix, again showing Rhat is not greater than 1.1 on all the variables. Figure 3.6 shows the traces beginning to mix as the iterations reach the end of the burn-in phase, and examination of the later iterations show excellent mixing.

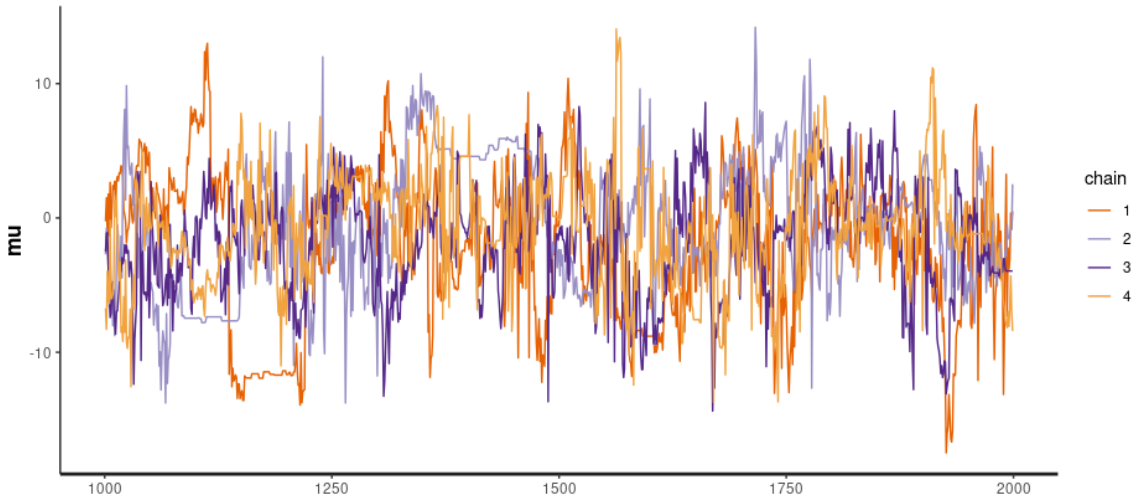

Figure 3.6: Trace Plot for the Two Level Model for temperature, for the duration of the burn-in phase. Note that the model appears to have begun mixing by the final 500 steps.

Two Level Model Posterior Density

The density estimate of the 2 level model posterior distribution in Figure 3.7 appears to have at least 2 peaks, with a primary peak at around approximately 0 and a second peak where μ is approximately -5. This indicates that the within-station and between-regions posterior is not well modeled by a unimodal distribution. This might be due to regional variability in the data.

Hence, we will explore the regions more carefully to identify possible sources for these modes. To do this, we performed single-level Bayesian modeling on each of the regions independently and checked their posterior density function to determine which may be influencing the 2 level model. To be clear, the more than one mode in Figure 3.7 indicates that some regions may have specific dynamic changes to their climate systems at differing locations from one another, and suggests Canada as a whole cannot be summarized from a single normal distribution with a single mode.

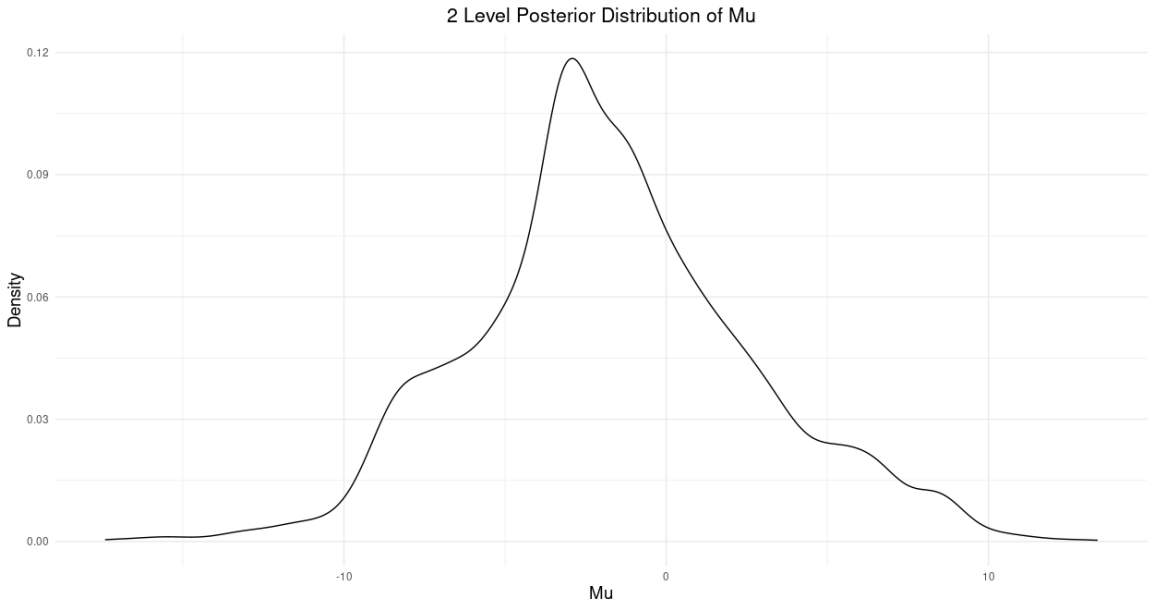

Figure 3.7: Posterior Density for the Two Level Model for Average Temperature Rate of Change (μ), all indices merged.

Which regions have More than 1 Mode?

There may also be specific regions that are clustered at more than one mode, which we will examine in Figure 3.8, which shows the posterior plots from the single level model for all six regions. This plot indicates that British Columbia and (to a lesser extent) the Prairies (Alberta, Saskatchewan, and Manitoba) each have more than one mode. The result for British Columbia corroborates the statement made by Stahl *et al.* [70] that: "British Columbia, Canada, is a domain with a complex topography and highly variable density and elevational distribution of climate stations". Due to the complexity in air temperature observed in British Columbia, Stahl *et al.* published a paper that compared approaches for spatial interpolation of daily air temperature in a large region with complex topography and highly variable station density. Similarly, the Prairies is a combination of 3 different geographic topographies that are bound to have varying and complex climatic conditions when brought together. Hence, regions

1 and 3 appear to be multi-modal, which, combined with the differing centralities of the regions is sufficient to have produced the pooled national plot observed above.

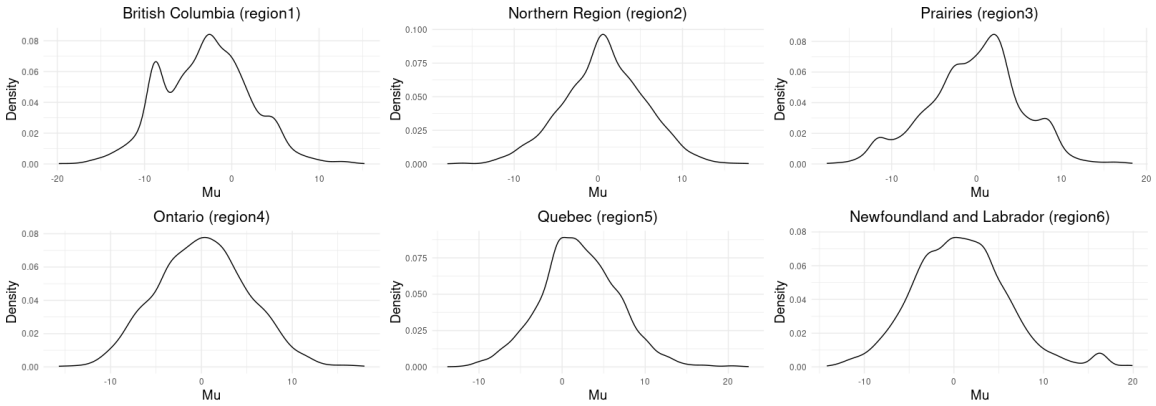

Figure 3.8: Posterior density plots for each of the regions independently modeled using the single level model.

Average Temperature Change at each Split Index for 2-Level Model

Now consider pooled by index, using the two level framework. The results are shown in Figure 3.9. The national mean change in average temperature for each of the indices looks to be approximately on the same level throughout the indices, at least relative to the credible interval. However, the credible interval seems to be quite large, which is probably due to the multi-modality and unusual regional influences on the slope that increase the joint variability. Additionally, note from Figure 3.7 that in the nationally pooled two level model, the mean is at -1.3 (i.e., -0.0013), similar to the single level model estimate, and again negative. But in Figure 3.8, we again see that there are only a few of the indices where the trend is downward. This likely has a similar root cause as in the single level model case, and also suggests that the

results are not representative, which matches our observations in Figure 3.8.

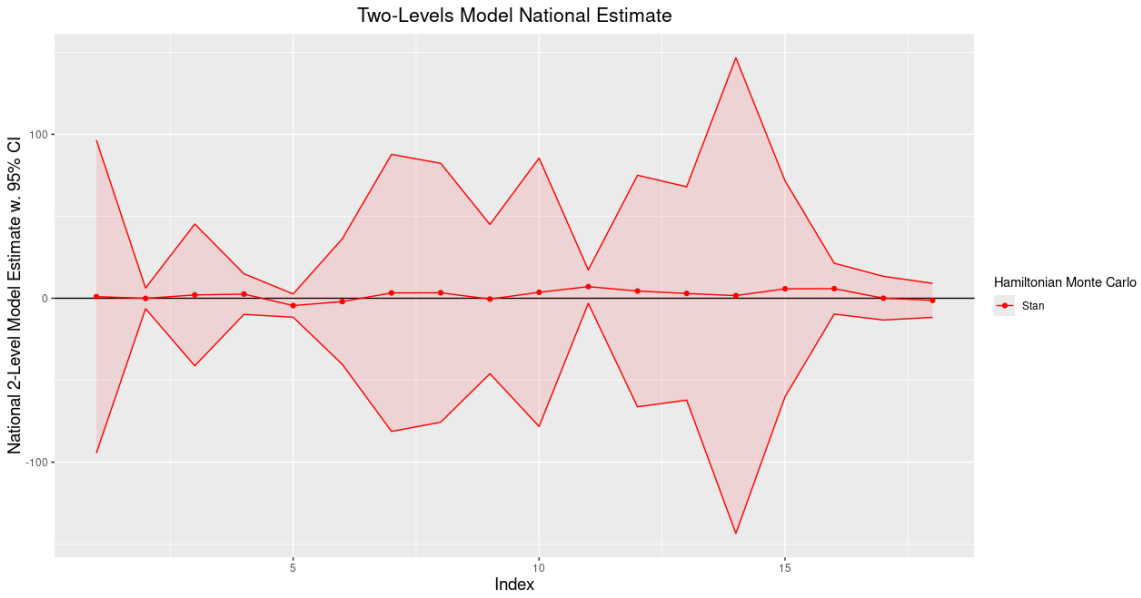

Figure 3.9: Two level posterior mean change for average temperature for each index (μ).

3.3.2.1 Regional Posterior Median Change in Average Temperature at each Split Index

Recall that we are multiplying the slopes (and standard errors) by 1000 before entering them into the Bayesian framework, to ensure numerical stability in the Monte Carlo draws. So all numbers in Figure 3.10 should actually be interpreted as $\times 10^{-3}$. Additionally, to stabilize the results somewhat, we are extracting the posterior *medians* in the following, rather than the means. The figure shows that British Columbia (region1, in red) has a significant number of negative trends across indices compared to the other regions, implying that British Columbia possibly has significant movement of its colder seasons; by contrast, the Northern region (region2) appears to have significant indices of positive changes in temperature, meaning a possibility of a persistent increase in temperature in the region, leading to a warmer climate. Ontario

(region4) appears to have the highest change at index 14 which falls around October and the same index has the lowest mean temperature change for British Columbia, showing a wide disparity in temperature within the same period in these different regions. Notably, all the regions had spikes in the change in temperature at some point in each of the indices during the summertime. So, as discussed in the literature review: we are seeing changes in the extremes. Warmer summers (positive trends in the June/July/August indices across all six regions), but shifting seasons around the summer (negative trends for index 9 in Quebec, Maritimes, and Newfoundland), and some colder "early cold season" periods, especially in British Columbia and the Prairies. This latter set of results is a shifting of the seasons, with wintery weather starting earlier, but also ending earlier (almost all regions show positive trends in index 3, March).

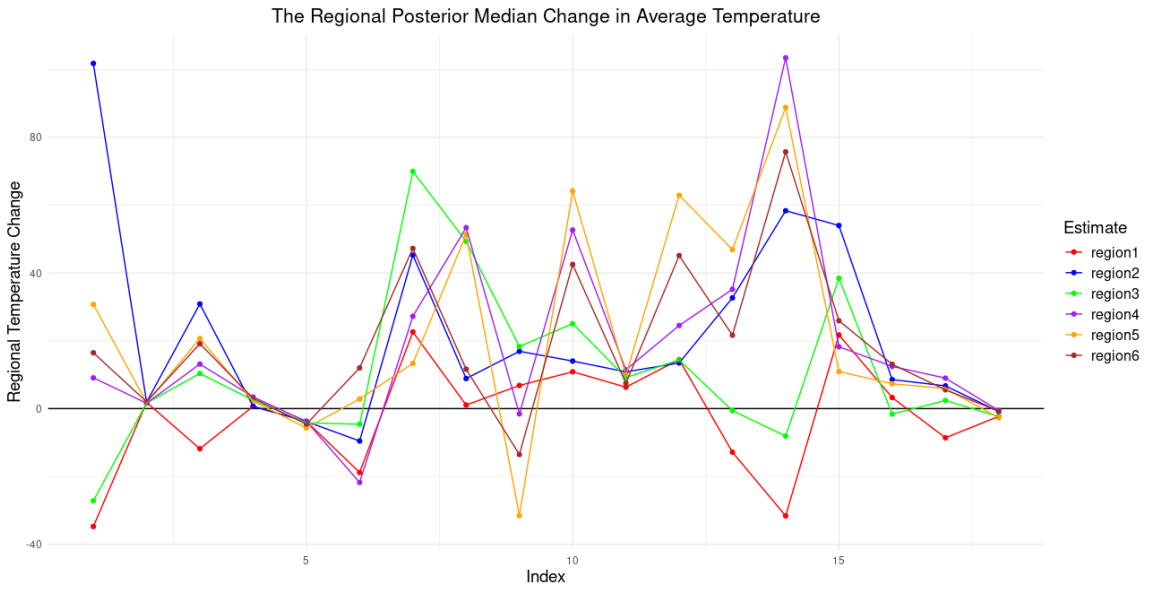

Figure 3.10: Regional Posterior median Change in Minimum Temperature Across 18 indices within 6 regions.

In the following subsections we will explore some specific split points where the regions are either similar and dissimilar, and discuss the implications for understanding

the evolution of the Canadian climate.

Regional Posterior Density Plots for Specific Splits

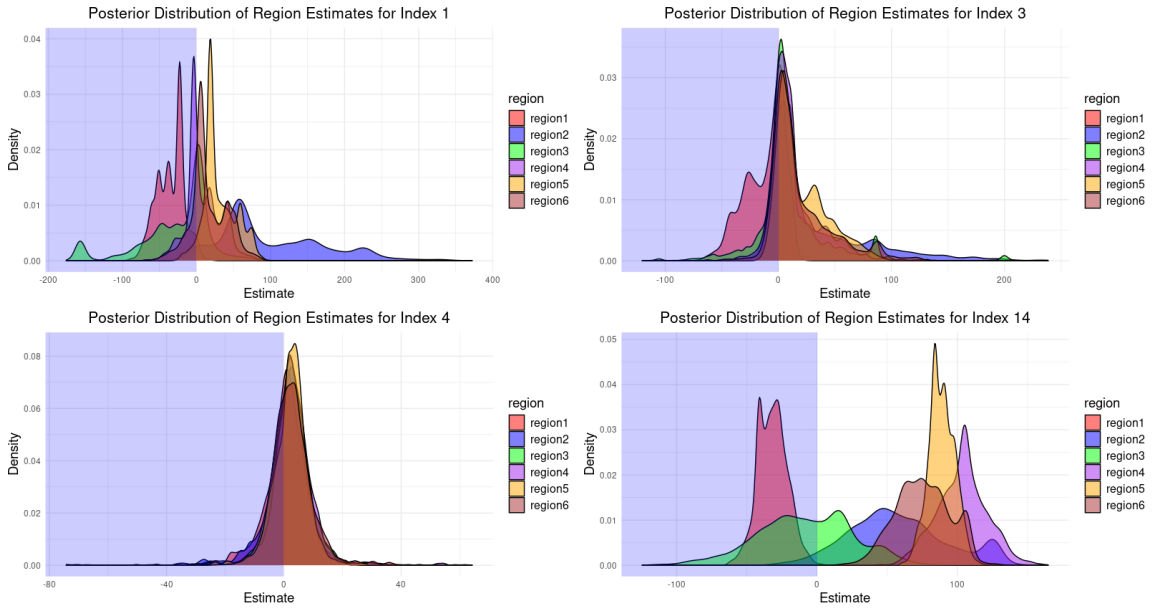

Figure 3.11: Regional posterior density plots for all 6 regions for split indices 1, 3, 4, and 14, chosen as those where the median trends were either very similar (4) or somewhat different (1, 3, 14). The light blue shaded backgrounds are a visual aide to easily see negative versus positive results - recall that these are slopes, so anything centred in the blue shaded region is a negative slope, indicating a downward trend in temperature.

It was observed that there was distinct behaviour in some regions within specific split indices in Figure 3.10. For instance, in index 1 (which happens to be the beginning of the year) British Columbia and the Prairies were quite negative. In Figure 3.11, we see that British Columbia has a multi-modal temperature distribution (red shaded density, entirely to the left of the cluster near the median). We also see that the Prairies (region 3, in green) are very elongated and low – this likely indicates widely varying station trends, such that the region is not consistent enough to estimate the density according to our model. There is a profound disparity in the temperature

distribution in the first few weeks of January in British Columbia, the Northern region, and the Prairies while the distribution in Ontario, Quebec, and Newfoundland are fairly similar with dominant central modes around the 0 mark.

In index 3 (top right facet, Figure 3.10), we see much more consistent results, with only British Columbia (region 1, in red) and the Maritimes (region 5, in yellow) having secondary modes of any significant size. All regions are positive in centrality (peak of the central mode), which matches the observed medians in Figure 3.11 for all but British Columbia. We can see the reason for the negative result in British Columbia: some set of stations have negative trends, sufficient to produce a bi- or multi-modal posterior, such that the median is situated between the modes and is drawn below zero. Thus, in March, much of the country is warming, consistently, across many stations, except for part of British Columbia which is actually getting colder. This may indicate seasonal drift in British Columbia.

By comparison, towards the later part of the year for index 14 (which is in the autumn in Canada, approximately October), there is a visible difference in temperature distribution across all regions. The plot for index 14 (bottom right, Figure 3.10) shows a profound inconsistency and variability in the weather conditions in terms of temperature. Most of the regions show warming temperatures, except for British Columbia and the Northern region with very different patterns in their variability.

Further observation of Figure 3.10 shows some extreme posterior temperature estimates; we will explore slopes at these index points to inform the probable cause of these extreme temperature estimates.

3.3.3 Checking for Pattern of Values in Regional Slopes

To explore the possible reasons for some of the patterns we observed above in some regions for some indices, we go back to the source data that is used to generate the

slopes, which in turn generate the likelihoods that lead to the posterior densities for regional trends.

Checking for Pattern of Values in the Northern Region

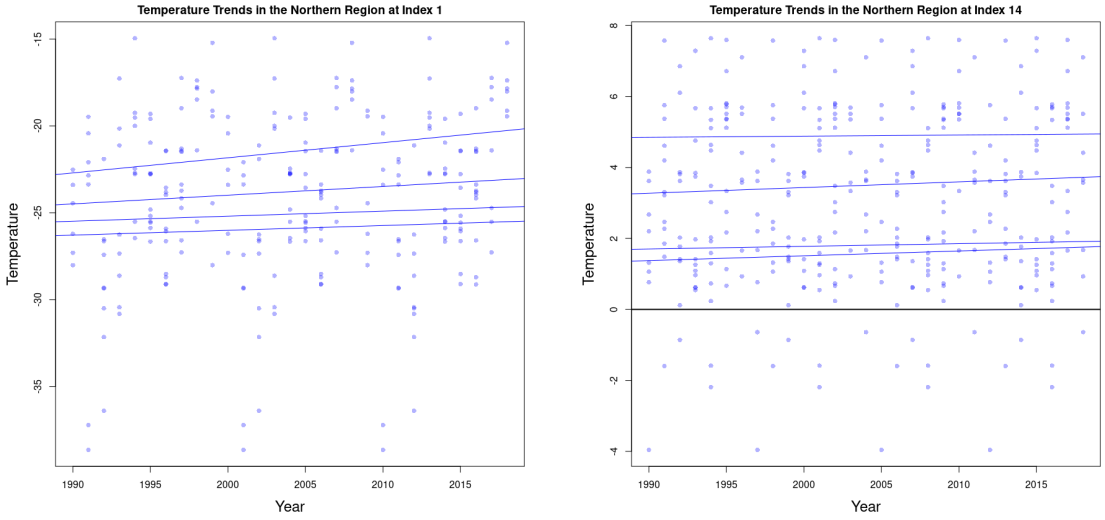

Figure 3.12: Spark plots of indices 1 and 14 for the Northern region to check if extreme slope values are in each of the stations. Each dot is a station-index hourly average, and the lines are the trends per station across the years (x-axis).

Firstly, we note that there were only 4 stations with sufficient data for this region; and 4 stations in a large region as the Northern region is insufficient to make concrete assumptions about the general climate pattern in this region. However, checking the pattern solely based on this limited data in index 1 of Figure 3.12 (left facet) for the inconsistency that leads to the somewhat large value seen in Figure 3.10 does not give an obvious answer. However, we do see that the slopes are fairly spread out, which does explain the spread nature of the posterior density in Figure 3.11. And as all the slopes are positive in the left facet, we would expect a posterior median to be positive; similarly for index 14 (right facet), we expect a somewhat spread out yet positive posterior. And this is what we had.

Checking for Pattern of Values in Regional Slopes (British Columbia)

As discussed earlier, British Columbia exhibited some non-standard patterns of behaviour at certain indices. And in Figure 3.13 we start to see why.

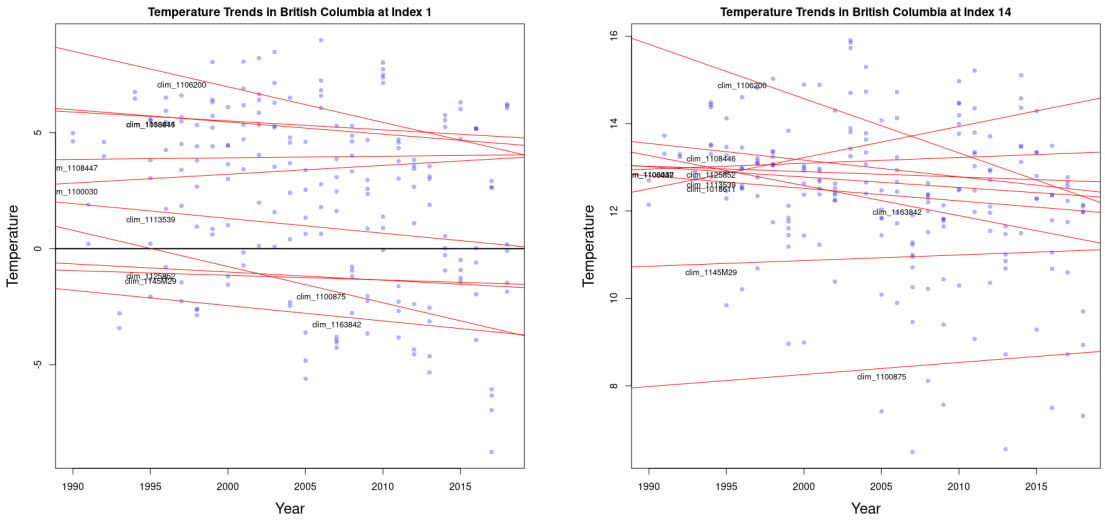

Figure 3.13: Spark plots of indices 1 and 14 for British Columbia region to check if extreme slope values are in each of the stations. Similar setup to Figure 3.12.

Figure 3.13 for British Columbia appears to have an extreme slope for station "clim1106200" in index 14 that influenced the negative movement of the posterior estimated slope for that index in Figure 3.10. This station is situated in Point Atkinson in British Columbia. This might be due to outliers, so we dig deeper, and look at this station in particular.

Outlier Check for Station clim1106200 (Point Atkinson)

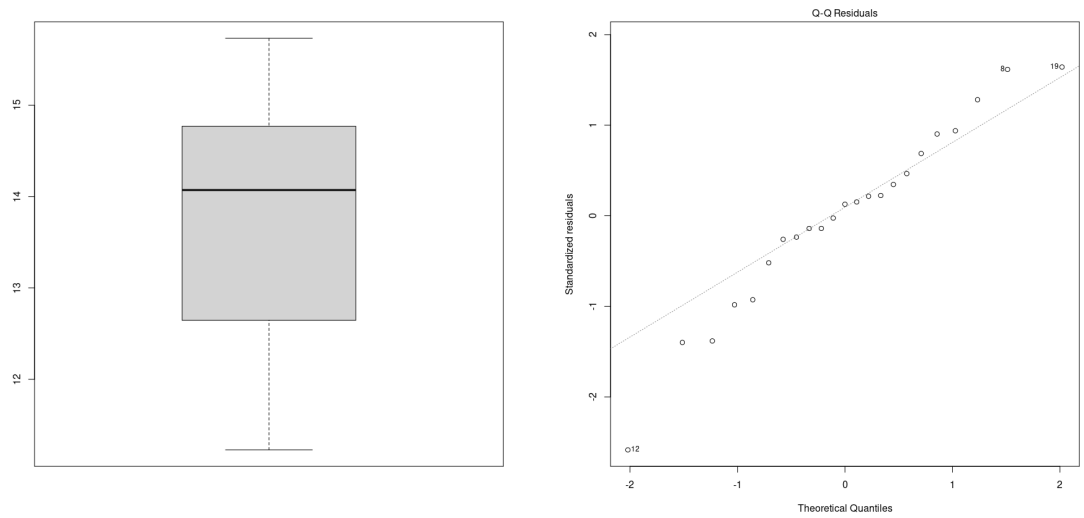

Figure 3.14: Box plot and QQ plot checking for outliers in station clim1106200 located at Point Atkinson in British Columbia. All inputs are sample averages of hourly temperature for index 14 (early October) for given calendar years.

The plots indicate that there are no obvious outliers in the data from the station in Point Atkinson, although the data is perhaps heavy tailed. This indicates there has been a profound change (reduction) in temperature in Point Atkinson during the study period for this time index (early October). Point Atkinson is located in southwestern British Columbia, specifically in West Vancouver, along the waterway that leads to Vancouver Harbour. The area is distinguished by its steep, rocky cliffs and the dense coastal temperate rainforest typical of the Pacific Northwest. These geographical features likely contribute to the site's mild and distinct variations in temperature. And effectively, what we are seeing in this trend is the early onset of winter conditions (such as they are for this sub-tropical climate zone) – the shifting of the seasons.

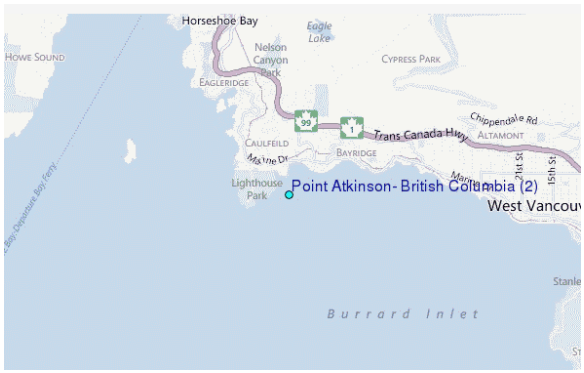

Figure 3.15: Map of Point Atkinson, near Vancouver, British Columbia, Canada.

A review of similar spark plots for the other regions did not show any suggestions of where specific large slopes influenced the direction of the posterior slope for a particular index.

3.3.4 When do we have the same weather across Regions?

One of the open questions we began this research hoping to answer was when regions have similar climate change impacts, and when they do not. This will allow us to establish "digital twins" for some selected times and regions, which may be useful in the establishment of climate change-based risk models in the future. In Figure 3.16 we examine four additional time indices, two where the behaviour is very similar across all six regions, and two where the behavior is wildly different.

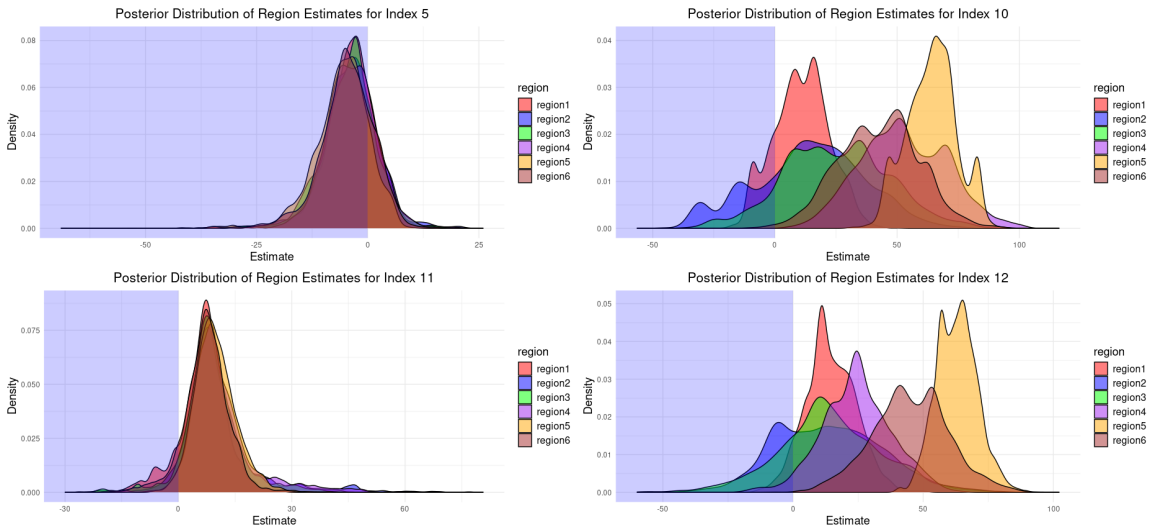

Figure 3.16: Regional posterior trend densities across indices 5, 10, 11, and 12 showing where temperature conditions are the same (5 and 11) and also profoundly different (10 and 12).

Figure 3.10 shows some indices where temperatures are the same, and others where they are profoundly different, while Figures 3.11 and 3.16 emphasize these points. Figures 3.11 and 3.16 clearly demonstrate that temperatures are consistent across regions at index 4, corresponding to approximately March, and at index 5, which aligns with April. Later in the year, at index 11 (which corresponds to August) the same consistency in temperature across regions is observed. This suggests that temperatures in Canada tend to be uniform across regions during the transition into, or out of, the summer season. Meanwhile, there are quite inconsistent temperature trends in other periods of the year, indicating differing impacts of climate change based on geography.

3.3.5 Conclusion

This concludes our development of a pipeline for examination of trends in climate metrics by station and index across Canada. As the reader can see, this is a flexible

framework, allowing an analyst to choose a metric of interest, and then develop regional and national estimates of the posterior median trends. Where these are coherent, we can conclude that nationally there are quite similar trends in the climate metric (e.g., trends in average temperature), while in the indices where they are incoherent or different in some systematic way, we can obtain valuable insight in the regional and geographical differences.

We believe this approach, with its flexibility and structure simultaneously, is a valuable contribution to the understanding of climate change in Canada, and should have significant dividends moving forward for analysts interested in the impacts of climate change on a number of other disciplines, especially population health and pollution.

3.4 Analysing Temperature Variations with other Metrics

As mentioned above (and earlier, in the methodology chapter), this pipeline can be applied to any chosen metric. Means have been used in the initial development to comprehensively demonstrate national and regional variations in temperature using the described pipeline in the methodology; below, we will exhibit the use of the approach on minimum, 10th percentile, 90th percentile, and maximum metrics of temperature. Recall from the literature review earlier in this thesis that climate scientists expect the extremes to be even more sensitive to climate change, so we expect to see increasing differences in regions and stronger trends across time for some of the extreme value statistics chosen in the following.

3.4.1 Using Minimum Hourly Temperature

For our first example, we consider minimum hourly temperature, again for 18 indices across the calendar year. All other aspects of the pipeline remain the same: estimate the metric (minimum); then compute a trend across years by station; then pool. Figure 3.17 shows the key results.

Figure 3.17 has national (black line, top facet) and regional (coloured lines, top facet) posterior estimates of change in minimum temperature for the study period. The national estimate showed that the most positive posterior median trend for minimum temperature occurred in the 10th index which is in the middle of summer. Using this metric, it is generally noticed that almost all regions are warming on almost all indices. Some unusually large results: all regions except region1 (British Columbia) experienced very large trends in minimum temperature across the study period for index 3, while all but British Columbia and the Northern region experienced the same for index 7. In the later part of the year (indices 13, 14, and 15), there is a tremendous amount of positive trends again – minimums in late summer and early fall are up quite a bit. Interestingly, the behaviour for indices 16, 17 and 18 are largely flat: minimums in early winter are essentially the same as they have been, with almost no trend.

The posterior density plots for the regions show that, most of the density distributions are multi-modal, although the strength of the secondary modes differs. This indicates some sub-clusters within the regions for the behaviour of the trends in mimimum temperature, possibly associated with latitude, although we do not have enough data to truly tell. A general regional observation about the variations in the trends for minimum temperature is that most of the regions have at least one positive mode, indicating that at least a subset of the stations in that region are experiencing warming trends: increasing minimums over time, slowly excluding colder results.

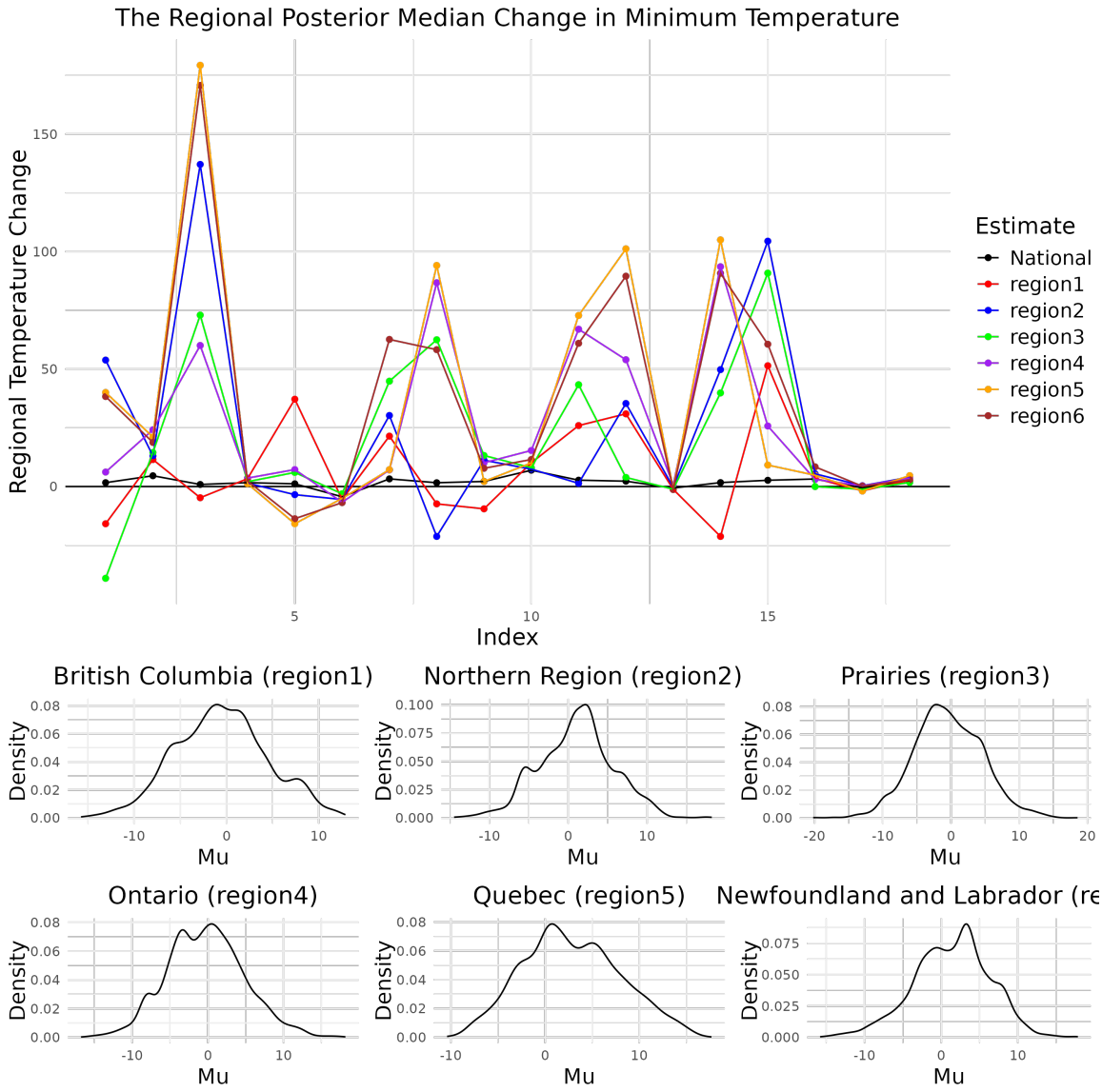

Figure 3.17: National (black line, top facet) and regional (all other lines and densities, bottom facet) posterior median change in minimum hourly temperature across 18 time indices in Canada and 6 regions.

3.4.2 Using 10th Percentile Temperature

The results for the 10th percentile are quite similar, and we apply the same methodology as for the mean, and the minimum.

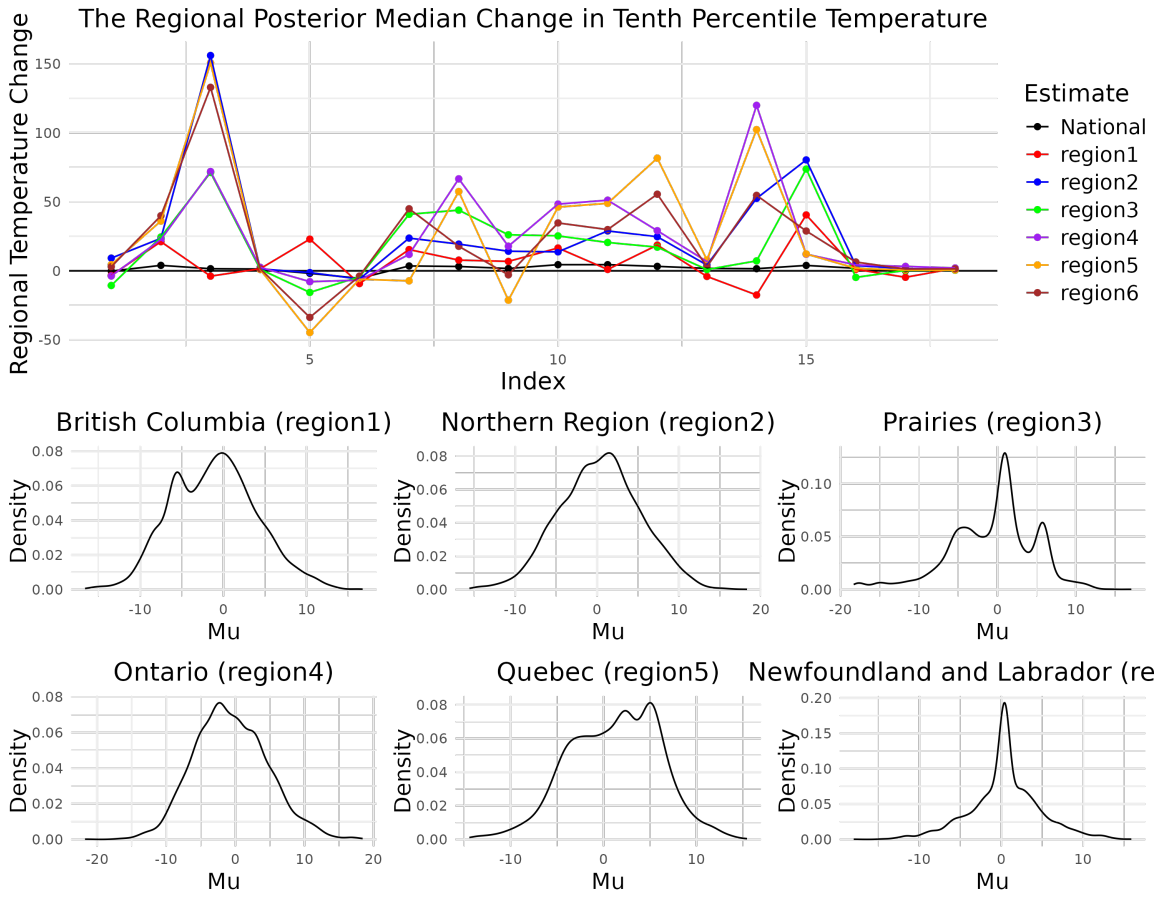

Figure 3.18: National and regional posterior median change in trends for the 10th percentile of hourly temperature across 18 indices in Canada and 6 regions.

Compared to Figure 3.17, the values for Figure 3.18 appear to be less multi-modal

and with less variation across regions. The obvious observation in these regions and the national estimate is that very few indices and regions are on the negative rate of change in 10th percentile temperature across the split indices, with a profound positive spike on the 3rd index for some of the regions. This again emphasizes warming regions across most of the indices for the lowest temperatures – the 10th percentile is increasing across time, drawing up the tail. However, the posterior densities of the regions show some multi-modality, suggesting some differences in behaviour for the 10th percentile of temperature in the climate stations in each of the regions.

3.4.3 Using 90th Percentile Temperature

Similar to Figure 3.18, Figure 3.19, the posterior density plots for each of the regions have some multi-modality. However, there are more negative trends in the this metric, possibly indicating seasonal shifting: especially indices 3 and 4, and then 18. In these cases, the warmer temperatures are trending down. This can indicate delay of the onset of spring in some regions, or the shifting earlier of colder (e.g., polar vortex) temperatures in some of the early-to-mid winter months.

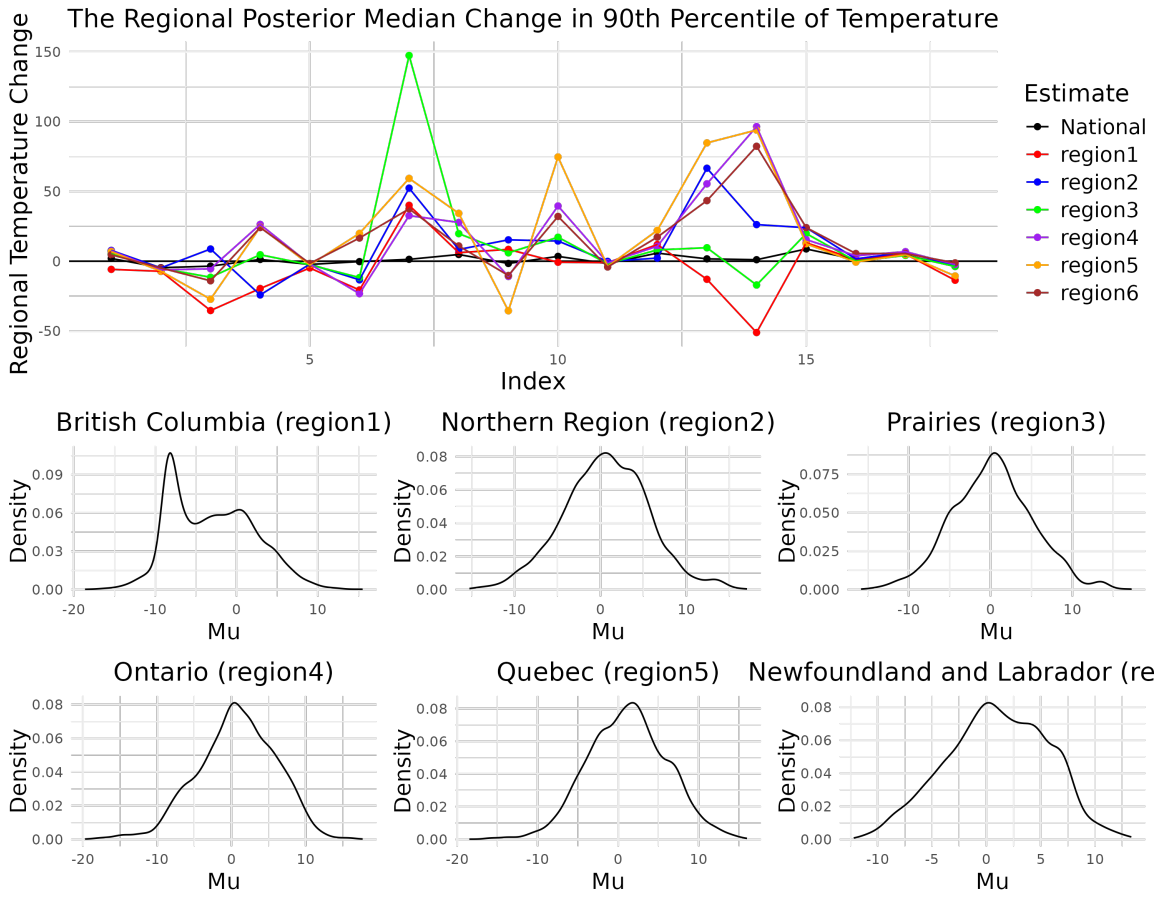

Figure 3.19: National and regional posterior median change in trends for the 90th percentile of hourly temperature across 18 indices in Canada and 6 regions.

3.4.4 Using Maximum Temperature

In Figure 3.20, we see strongly positive trends in the late spring months (indices 7 and 8), and for some regions, again in the late summer months (indices 13 and 14). There is a strong dip in index 3 (March), indicating colder overall temperatures - less

balmy, warm late winter days - but slight increases in index 17, indicating increasing maximum hourly temperatures in the late fall, trending to early winter.

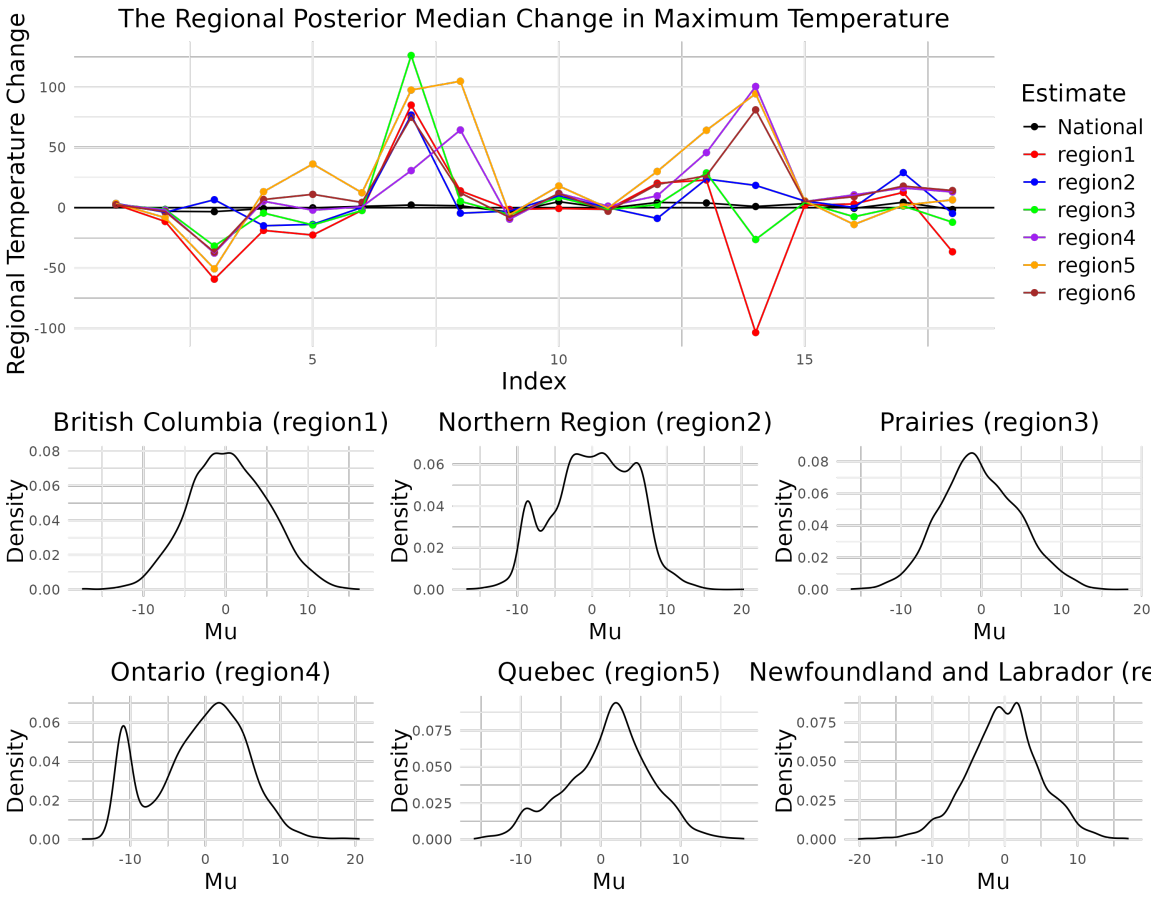

Figure 3.20: National and regional posterior median change in trends for the 90th percentile of hourly temperature across 18 indices in Canada and 6 regions.

3.5 Conclusion

In this chapter, we developed a complete pipeline, from hourly data at the station level, to regional and national pooled estimates of posterior densities of trends. This method allows us to examine the regional and national estimates of changes over time in chosen climate metrics. While all of our examples were chosen from temperature, this was mainly due to the widespread availability of temperature, and the methods could easily be applied to any similar hourly data chosen to be of interest.

4. *Time Series Data Clustering*

Clustering (in an unsupervised sense) is a general algorithmic approach that aims to identify structure in an unlabelled data set by objectively organizing data into homogeneous groups where the within-group-object similarity is maximized and the between-group-object dissimilarity is maximized [46]. It can be considered as a data mining technique where similar data are placed into related or homogeneous groups without advanced knowledge of the groups' definitions [64, 1].

In this thesis, we have worked extensively with time series data, developing in the previous chapter a pipeline for analysis of massive multivariate geographically separated time series of hourly climate data. Now, we wish to consider whether the results (at a variety of pooled levels) can be clustered in order to identify "digital twins" – stations or regions in Canada that behave similarly, despite possibly being quite geographically separated. For example, perhaps a station on the Pacific coast might have more in common (climate change trend-wise) with a station on the Atlantic coast, than either has in common with stations deep in the interior of Canada.

4.1 Categories of Clustering Analysis

In general, some authors classify clustering methods into five major categories: partitioning methods, hierarchical methods, density-based methods, grid-based methods, and model-based methods [25]. We will examine these, and decide on methods that

are useful for our purposes.

4.1.1 Partitioning Clustering Method

The partitioning method of clustering involves having a set of n unlabelled data tuples and k partitions of the data are then constructed where each partition represents a cluster containing at least one object, with $k \leq n$ (the data size). A partition is classified as *crisp* when each object is assigned to only one cluster. In contrast, in a *fuzzy* partition, an object can belong to several clusters with different degrees of membership. Two widely recognized crisp partitioning methods are **k-means** and **k-medoids** algorithms. In k-means, each cluster is represented by the average value of the objects within it, while in k-medoids, each cluster is defined by the object that is most centrally located [49, 43].

4.1.2 Hierarchical Clustering Methods

This clustering method groups data objects into a tree-like structure of clusters. There are two main types of this method: **Agglomerative** and **divisive** clustering. Agglomerative methods start by assigning each object to its own singleton cluster, and then progressively merge these clusters into larger ones. This process continues until all objects are combined into a single cluster or a stopping criterion, like a specified number of clusters, is met. Divisive clustering on the other hand does just the opposite of what agglomerative clustering does: starts with one single cluster, and divides until the stopping point is met.

4.1.3 Density-Based Clustering Methods

This clustering method expands a cluster as long as the density within the surrounding area surpasses a specified threshold. This is a non-parametric approach where the

clusters are considered high-density areas of the density $p(x)$. A density-based cluster is a set of data objects spread in the data space over a contiguous region of high density of objects, separated from other density-based clusters by contiguous regions of low-density objects [11]. An example of a density-based algorithm popularly used for clustering is **DBSCAN**.

4.1.4 Grid-Based Clustering Methods

This approach divides the data space into discrete cells, and then performs clustering operations within this grid structure [84]. The clustering depends on the number of grid cells and is independent of the number of data objects [53]. An example of this is the Statistical Information Grid-based (**STING**) clustering method [84], which was proposed as a way to cluster spatial data in such a way that the spatial area of the data is divided into rectangle cells at different levels of resolution, forming a hierarchical structure. In this case, the statistical information of each cell is calculated and stored beforehand and then used to answer spatial mining queries [87].

4.1.5 Model Based Clustering

This family of clustering methods assumes a model for each of the clusters and attempts to best fit the data to the assumed model. For this method, the statistical approach uses either Bayesian statistical analysis to estimate the number of clusters [12] or a Neural Network approach to clustering. There is a lot of active research in this area, with a good summary up to 2016 covered in McNicholas' monograph [52].

4.1.6 Time Series Clustering Algorithms

Numerous algorithms have been proposed in the literature for time series clustering. However, most of these methods are primarily designed for static data, with adaptations for time series often developed based on those original static data algorithms. The approach of handling time series data in a similar pattern as that of static data usually works on raw time series data – this usually works by converting a raw time series data to either a feature vector of lower dimension or several model parameters and then applies a conventional clustering algorithm to the extracted feature vectors or model parameter. This is called feature-and-model-based approach [46]. However, in isolation, there are three main algorithms for analyzing time series data: raw-data-based; feature-based; and model-based algorithms. The raw-data-based involves clustering raw time series data, the feature-based is performed by extracting features from the raw time series data before clustering based on the features while the models based is done by either discretizing before modeling or modeling directly and then extracting model features like coefficients or residuals that is eventually used for the clustering.

4.2 Clustering Canadian Temperature Time Series

The raw time series data for this clustering was processed according to the procedures detailed in Section 3.1.1. As a demonstration of the proposed process of clustering temperature variability across Canada, Hierarchical Agglomerative clustering analysis described in Section 4.1.2 was performed on the mean[1] of each of the 18 split indexes from the raw data. These means were computed by iterating through all the years in each split index and then, computing the mean value for each of these splits. These

[1]That is, only the averages: no trends, just simple hourly averages.

computed means serve as feature vectors for the data set and are ultimately used to create the clusters. Then, the clusters are graphically represented on the Canadian map using differing numbers of clusters k to show the regional clustering of the average change in temperature in Canada.

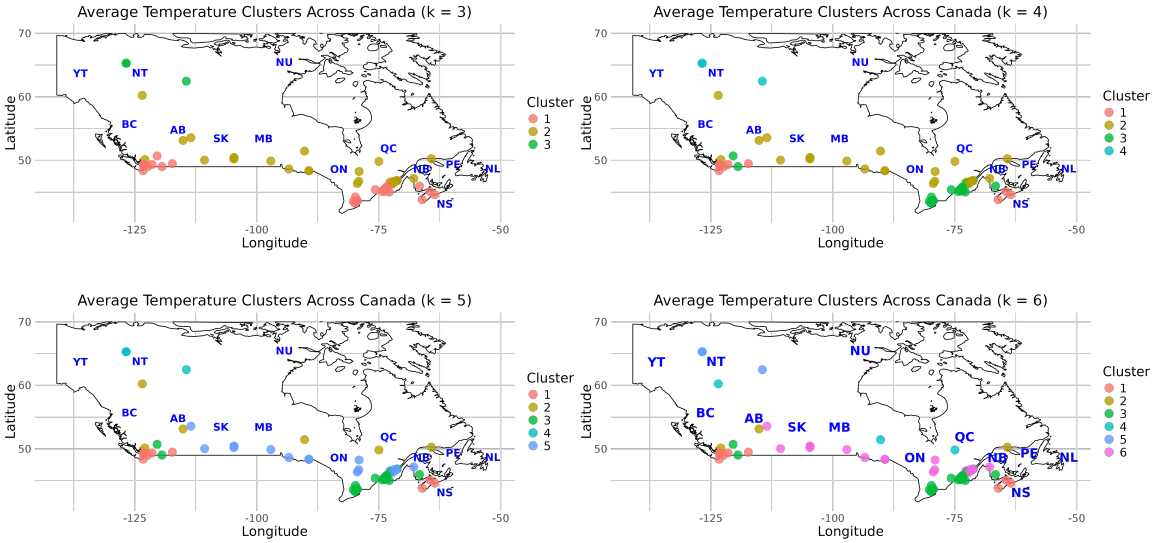

Figure 4.1: Canada's map with cluster identified stations across different regions. clusters k = 3, 4, 5, and 6 in the four facets of the plot.

Figure 4.1 shows that there are clustered average temperatures across different regions and show a flow of the same clusters from East Central to the Prairies for all four groups of clusters. Do note that this example is intended to show how the result of our interested metric will be presented in the following, and not to demonstrate anything in particular about average temperature across regions. The main focus of this chapter is to explore temperature variability with the average median *change* in temperature across regions and to determine if there are similarities in this change in different regions to provide a better understanding of change in climate in Canada.

4.2.1 Feature-Model-Clustering Algorithm for Temperature Variability in Canada

The clustering of Canadian temperature data was conducted by integrating all the methods outlined in 4.1.6. This involved segmenting the data into multiple windows and estimating the slopes within each window using the specified modeling approach from the previous chapter. These slopes, serving as feature vectors in aggregate, were then input into the hierarchical agglomerative clustering algorithm described in 4.1.2. The clustering algorithm effectively grouped the temperature data into meaningful clusters based on the feature vectors. This approach employed the Feature-Model-Hierarchical clustering method, which integrates a model-driven approach, feature vectors, and the agglomerative clustering technique to achieve the desired clusters.

The slopes estimated by using the different desired metrics of mean, minimum, 10th percentile, 90th percentile, and maximum for the model were also clustered and shown on the Canadian maps in the following.

4.2.2 Clustering Mean Temperature Trends

Unique regional characteristics play a significant role in shaping how climates change over time, as introduced in the literature review at the start of this thesis. Factors such as geography, topography, and proximity to bodies of water can cause climate patterns to vary widely between regions. For example, islands often experience distinct climatic influences compared to tropical regions. Islands are typically more affected by oceanic currents, which can moderate temperature fluctuations, while tropical regions are more directly impacted by solar radiation, leading to warmer and more stable temperatures.

However, when conducting a deep clustering analysis of climate data, some unexpected similarities might emerge between these seemingly contrasting regions. This can be attributed to microclimaticc factors —- such as local wind patterns, elevation, or vegetation —- which can influence temperature dynamics in subtle ways over time. Despite the broader climatic differences, clustering techniques can reveal shared patterns at a granular level, suggesting that even regions with stark geographic or climatic differences might exhibit comparable trends in certain environmental variables due to these underlying factors. By incorporating advanced clustering methods like this one, hidden relationships in average temperature patterns across diverse regions in Canada were uncovered, offering valuable insights into how global and regional forces interact to shape climate change.

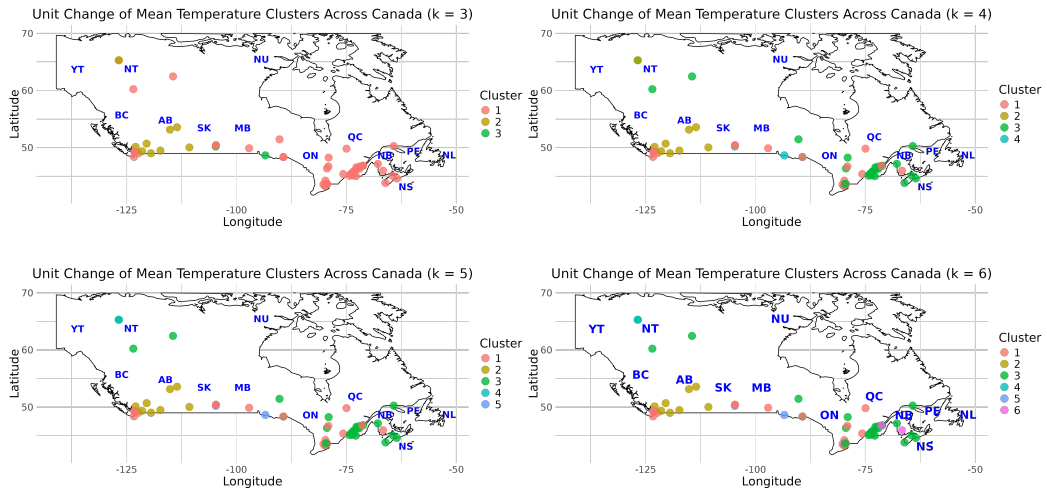

Figure 4.2: Canada with clusters of estimated slopes (change in average hourly temperature over time) for the metric of mean temperature for each split index in different climate stations across different regions. clusters k = 3, 4, 5, and 6.

First, it is important to note the number k of clusters in the plot can influence the narrative of what can be deduced from the plot. The eventual different narratives derived from any given plot due to the number of cluster changes are still valid and

explain a *possible* scenario of how the climate is changing across different regions. A key observation in Figure 4.2 is that, across all cluster configurations (choice of k), stations with similar temperature changes over the period still tend to group together in regions, suggesting that geographic characteristics largely influence temperature trends.

In all four clusters in Figure 4.2, the algorithm identifies the Atlantic region as being quite dissimilar to the Prairies. The Atlantic region, with its coastal proximity to the Atlantic Ocean, experiences a maritime climate characterized by moderate temperature variations, milder winters, cooler summers, and frequent precipitation. In contrast, the Prairies are known for their flat, expansive plains and continental climate, which results in more extreme temperature fluctuations -— hot summers and cold winters —- due to the absence of the ocean's moderating influence. These differences may help explain the varying temperature trend clusters observed. Thus, these unsupervised clusters indicate that the trends in the Atlantic are more self-similar than those in the Prairies; or, in climate change terms, that climate change is impacting the trends in different ways in the two locations.

By contrast, some stations in the Northern Territories and the Atlantic region consistently fall into the same clusters across all configurations, indicating that the climate in the Northern Territories is exhibiting patterns of change similar to those in the Atlantic region. A similar clustering situation is also observed in the Western and Western Central Region; however, these individual pairs are notably different in all cluster configurations that are greater than three.

How the Clusters of Average Temperature Change are Different between Clusters Across Canada

To examine temperature trend variability across clusters in Canada, we generated box plots for all 18 split indices using $k = 4$ as a restriction. Other choices of k gave

very similar results when tested.

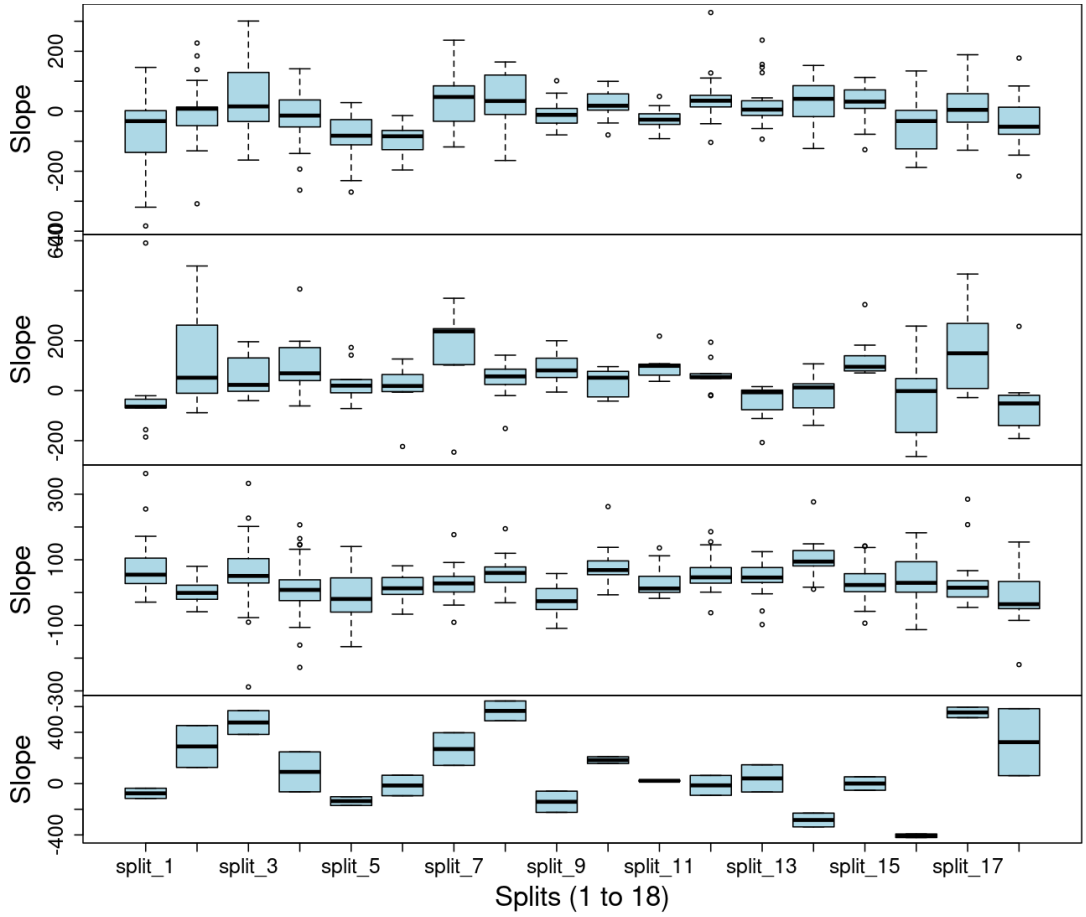

Figure 4.3: The distribution of the slope values of hourly mean temperature changes across 18 splits for each of 4 clusters from the $k = 4$ realization of the clustering algorithm. Cluster 1 to Cluster 4 from top to bottom facets in this plot.

For all of the following discussion, note that the cluster assignments are those visualized in Figure 4.2, top right facet ($k = 4$). Starting with cluster 1 which are the stations scattered primarily around Ontario region, but also the West Central and the Western Regions, the box plot shows reasonably high variability in the mean temperature trends during the earlier part of the year, shown by the earlier split indices (1-8). Additionally, several indexes show warming temperature trends, with predominantly positive slopes (e.g., indexes 10 and 12).

Meanwhile, in cluster 2, mainly gathered around the Prairies region, we can see some obvious differences from the first cluster (which is likely what the clustering algorithm is picking up on). More positive slopes in the early indexes, through to index 13, and then quite variable and negative slopes in indexes 16 and 18.

Cluster 3, which consists of stations that are largely clustered around Ontario and the Atlantic region, with a scattering of other stations in the North, similarly has some characteristics that are unique to the cluster. It is largely positive slopes in both the first and third index, and again at index 10, while all of 15-18 are more negative. Again, this is just indicating that the clusters *are* identifying common trends in selected indexes as indicative of similarity, and clustering around them.

The fourth cluster is arguably not important. It has 3 or 4 stations only, and simply appears to be chosen as being stations that do not belong in other clusters. If we were optimizing on the cluster size, this might be an indication that we should really be setting $k = 3$ instead, as there is nothing that stands out for these stations except possibly very large positive or negative trends in certain indexes (e.g., indexes 2, 3, 17 and 18 are very positive; indexes 14 and 16 are very negative).

4.2.3 Clustering of Minimum Temperature Trends

Some regions in Canada may experience similar degrees of change in cold temperatures over the study period, while others show notable differences. Figure 4.4 shows the clustering of regions based on the extent to which their minimum temperatures is changing.

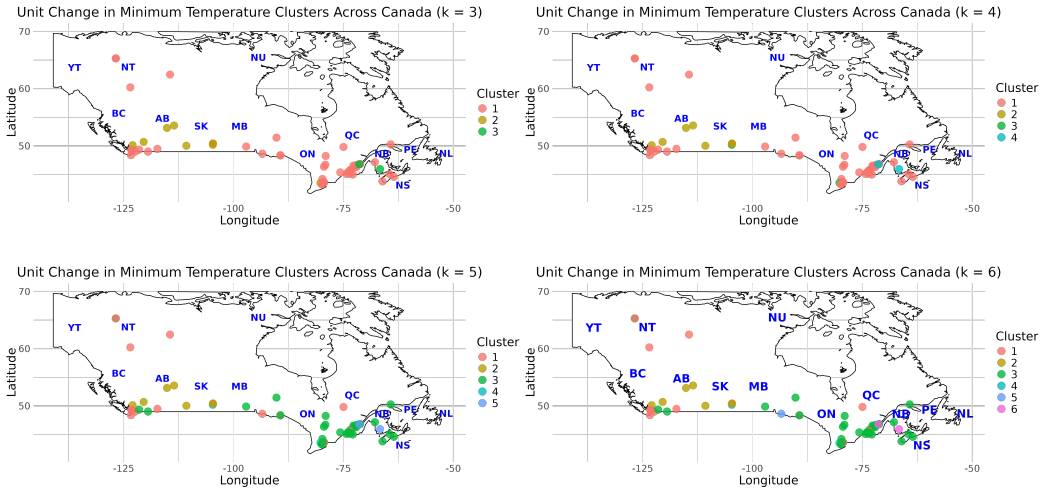

Figure 4.4: Canada with clusters of estimated slopes (change in minimum hourly temperature over time) for minimum temperatures of each split index in different climate stations across different regions. clusters k = 3, 4, 5, and 6.

Figure 4.4 shows that the Atlantic, West Central, Western, Quebec, and the Northern regions have approximately the same clustering for $k = 3$ and $k = 4$. However, when the clustering configuration was increased to 5 and 6, we see that the Atlantic and the West Central mostly share the same clusters while the Western region, Quebec, and the Northern Territories share the same clusters. Meanwhile, stations in the Prairies have completely different clusters across all cluster configurations. As with the mean hourly trend above, we again choose $k = 4$ to explore and explain, for continuity. However, in this example, it appears clear that there are at most 3 (and probably only 2) real clusters with sufficient data to identify, and if an analyst was interested in pursuing this example at a deeper level, adaptive control of the clustering number would be essential for interpretation.

How the Clusters of Minimum Temperature Change are Different between Clusters Across Canada

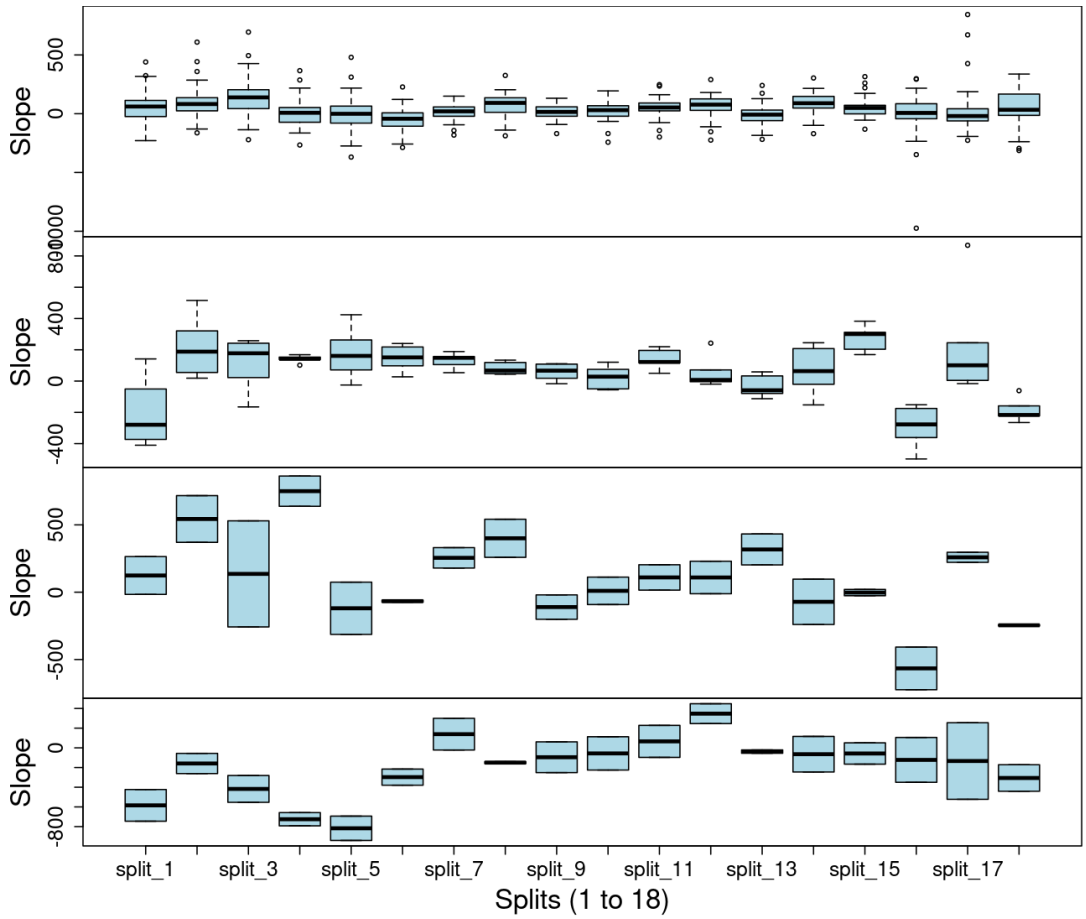

Figure 4.5: The distribution of the slope values of hourly minimum temperature changes across 18 splits for each of 4 clusters from the $k = 4$ realization of the clustering algorithm. Cluster 1 to Cluster 4 from top to bottom facets in this plot.

Figure 4.5 shows the distribution of change in minimum temperature in 4 cluster configuration over time. We can clearly see the lack of support for the third and fourth clusters in this plot, as the boxes are sets of at most 3 stations; these are simply stations with certain extrema behaviour that do not match either cluster one or two.

4.2.4 Clustering of 10th Percentile Trends

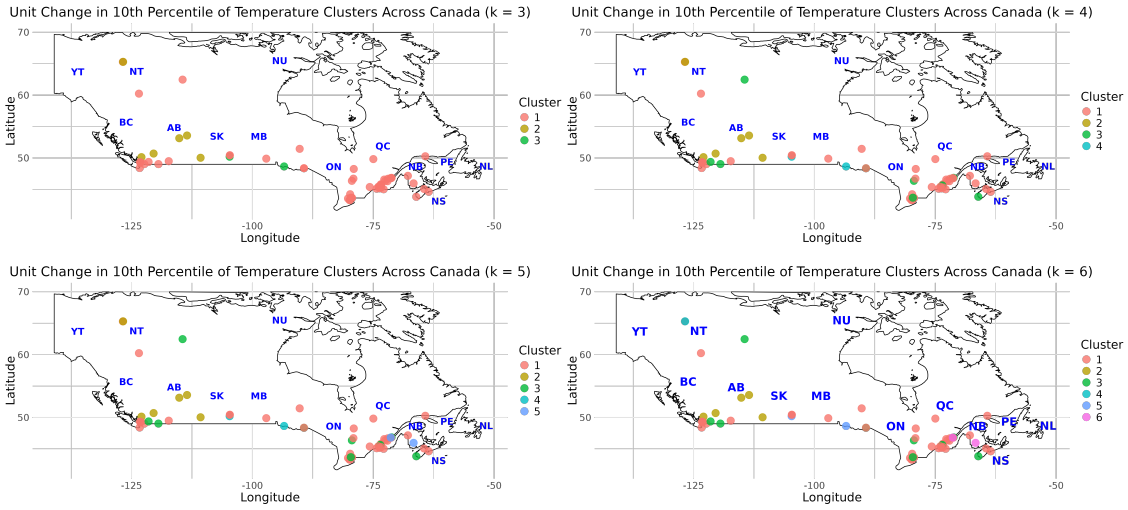

Figure 4.6: Canada with clusters of estimated slopes (change in 10th percentile hourly temperature over time) for temperatures of each split index in different climate stations across different regions. clusters k = 3, 4, 5, and 6.

Examining these clusters as we vary k, it appears that third cluster for $k = 3$ and the fourth cluster for $k = 4$ are very much "the leftovers" – stations that do not match the patterns of the others. There does not appear to be a clear break-point where the clusters follow recognizable patterns, except perhaps $k = 3$ where the behaviour seems to be "low latitudes" for the first cluster and "Prairies" for the second, while the third is erratic. However, interestingly, such a cluster puts two of the three Northern stations together with the bulk of the rest of the country, indicating some possible differences between the two stations in red and the single station that clustered with the Prairies. When $k = 4$, things become more spread and much less interpretable. It is not clear if this approach to clustering was valuable for this particular example.

How the Clusters of 10th Percentile Temperature Change are Different between Clusters Across Canada

Figure 4.7 shows 10th percentile temperature change trends across the 18-splits for 4 clusters, each panel representing the slope distribution for a different cluster. Again, we choose $k = 4$ not because it necessarily represents this particular set of data best, but for comparison purposes.

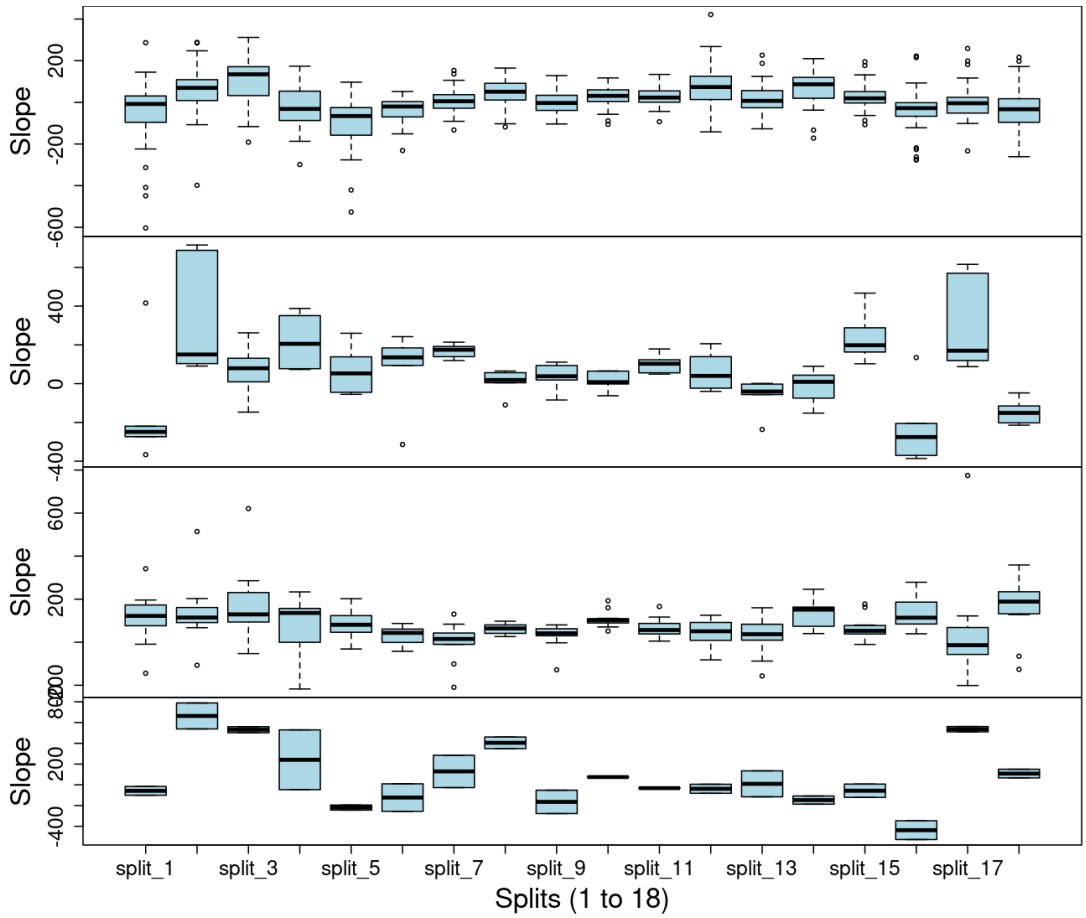

Figure 4.7: The distribution of the slope values of hourly 10th percentile temperature changes across 18 splits for each of 4 clusters from the $k = 4$ realization of the clustering algorithm. Cluster 1 to Cluster 4 from top to bottom facets in this plot.

Similar to cluster 1 in Figure 4.4, the cluster formed for the change in 10th percentile of temperature goes from the Atlantic to West Central and some parts of the Western and Northern regions. Since the 10th percentile takes care of some extreme values apparent in minimum temperature, the box plot indicates a consistent milder warming for cluster 1 by comparison, with peak warming in indexes 1-4: winter. This matches our earlier finding that the 10th percentile metric captures warming winters, which are less extreme in their cold weather on average.

The second cluster that is centred around the Prairies appear to have profound inconsistency in the nature of change in the 10th percentile temperature as it is observed that some locations have high positive slope while some have high negative slopes; suggesting that the 10th percentile temperature in these locations fluctuate across the cluster stations. In particular, this cluster appears to have captured high levels of erratic behaviour in warming for indexes 2 and 17, combined with steep decreases in indexes 1 and 16. Interpreted in colloquial terms, these stations share much warmer lows in early February and late November, combined with much colder lowers in early January and late October/early November. This may correspond to seasonal shifting: the coldest part of the winter moving to January from February would explain indexes 1 and 2, and the winter beginning earlier, but being more mild, would explain indexes 17 and 18.

Cluster 3 are locations around the Atlantic, West Central and Western regions, and this cluster generally show positive median slope with not much variation, suggesting slight warming temperature in the tenth percentile of temperature slopes but no distinctive features.

4.2.5 Clustering of 90th Percentile Trends

On the opposite end of the scale, we examine the 90th percentile of hourly temperature and their trends in Figure 4.8.

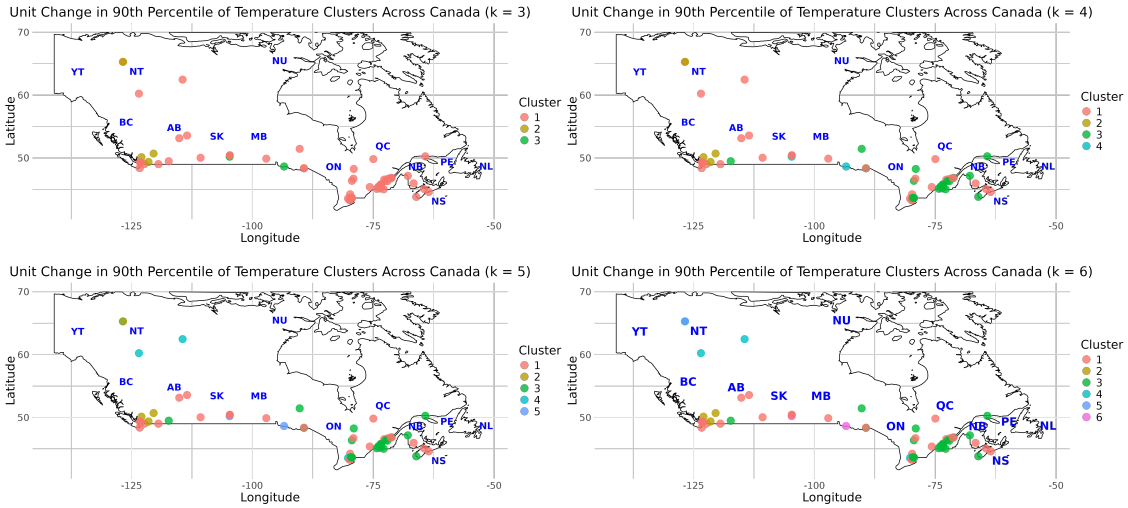

Figure 4.8: Canada with clusters of estimated slopes (change in 90th percentile hourly temperature over time) for temperatures of each split index in different climate stations across different regions. clusters k = 3, 4, 5, and 6.

Across all four cluster configurations in Figure 4.8, a subset of locations in Western Canada consistently form clusters, highlighting different trends in warm temperatures compared to other regions. This suggests that portions of the Western region experiences unique warming patterns. In contrast, the Prairies, and Quebec generally cluster together, indicating a more uniform trend in warm temperature changes across these regions. Meanwhile, the Atlantic and Western Central Canada regions exhibit a mix of clusters, pointing to greater variability and irregularity in its warm temperature trends during the warmer seasons, reflecting a less consistent climate pattern in that area.

How the Clusters of 90th Percentile Temperature Change are Different between Clusters Across Canada

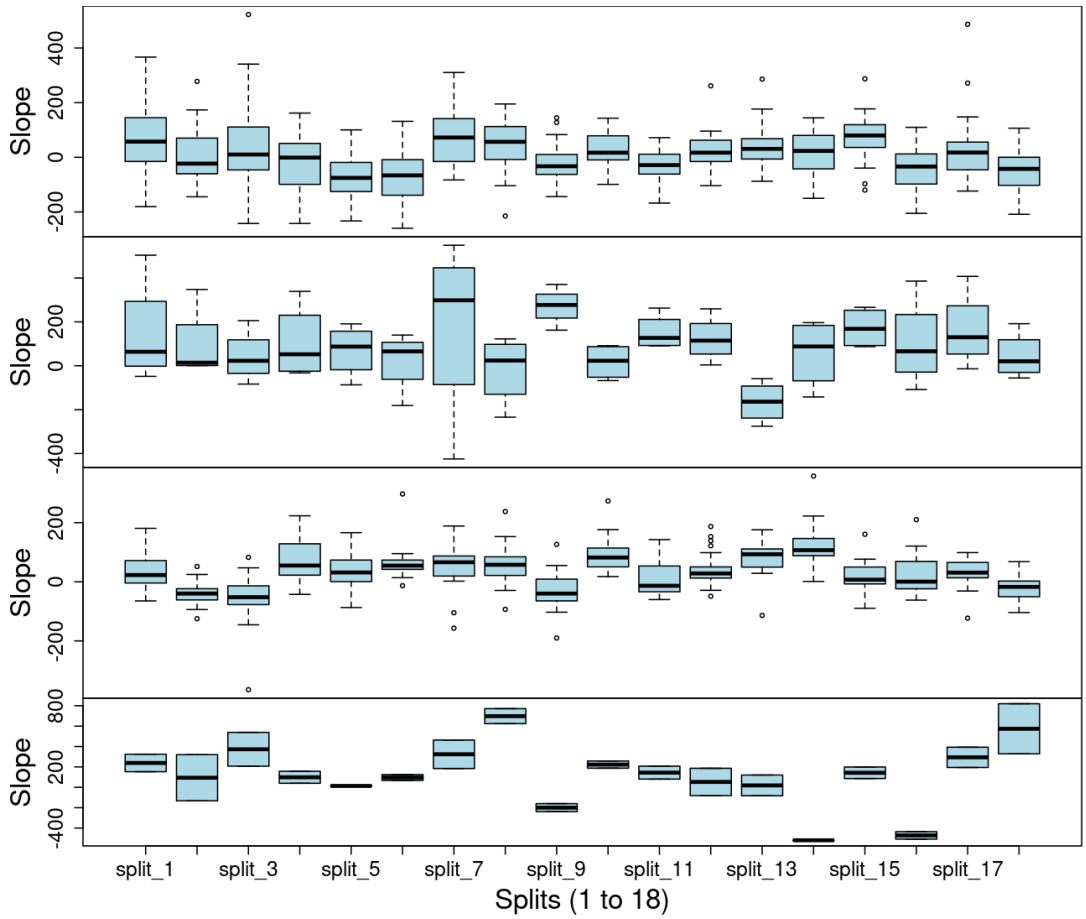

Figure 4.9: The distribution of the slope values of hourly 90th percentile temperature changes across 18 splits for each of 4 clusters from the $k = 4$ realization of the clustering algorithm. Cluster 1 to Cluster 4 from top to bottom facets in this plot.

Figure 4.9 shows 90th percentile temperature change trends across the 18 splits for 4 clusters, each panel representing the slope distribution for a different cluster. Again, $k = 4$ is chosen more for comparison purposes than for any particular matching of "best" choice for this data. Although, in this case, $k = 4$ may be the most interesting case, due to the splitting of the Ontario, Quebec, and Atlantic regions into multiple

clusters, and the isolation of the oddity stations in the fourth cluster.

Cluster 1, which cuts across practically all the regions in Canada, shows quite consistent slope values around zero; indicating little to no change in the 90th percentile of slopes with some minor variability across splits. There is an interesting downward pattern in indexes 1-5 (winter and early spring), and similar negative trends in indexes 16-18. This may indicate that these clustered stations are experiencing less high temperature hours and days during the winter.

By comparison to what is seen in terms of variability in cluster 1, cluster 2 (largely centered on the Rocky Mountains) exhibit some high variations with a mix of positive and negative median slopes identified on the box plot. Almost all of indexes 1-6 are positive, indicating warmer than usual high temperatures across the winter and spring, and indexes 9 and 13 are extreme. These latter indexes are the months surrounding summer, so we would associate these with much warmer late spring and early summer, warmer summers in general, but then a rapid drop in index 13 (early autumn) indicating less high temperatures in the transition to autumn.

The 3rd cluster is predominantly Ontario, Quebec and the Atlantic regions. The plot demonstrates narrow variability which emphasizes some consistency in the temperature trend with positive and negative slopes across splits. Many of these indexes are mildly positive, indicating consistently warmer "highs" in those months across the regions.

And finally, the fourth cluster is the outliers or oddities: stations that just don't fit into any other category, gathered together by the algorithm under the constraint that $k = 4$. This is useful in some ways, as setting $k = 3$ spreads these points across the other clusters, and produces less interpretable combinations of stations.

4.2.6 Clustering of Maximum Trends

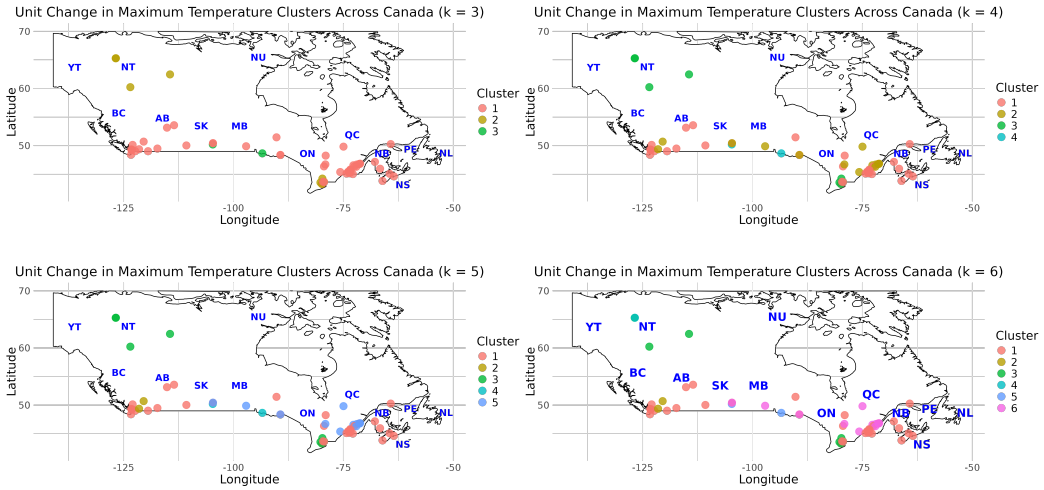

Figure 4.10: Canada with clusters of estimated slopes (change in maximum hourly temperature over time) for temperatures of each split index in different climate stations across different regions (Region1 = BC=Western region, Region2 = Northern region, Region3 = Prairies = [AB, SK, MB], Region4 = West Central = [ON], Region5 = West Central = Quebec, Region6 = Atlantic = [NS, PE, NL]; with the number of clusters k = 3, 4, 5, and 6.

With the modeling of maximum temperatures (by comparison to the 90th percentile, this would be no longer adjusted for extreme heat events), the clusters in Figure 4.10 resemble those in Figure 4.8, but with increased variability in the clustering patterns observed in the Prairies. This suggests that without accounting for extreme temperatures, the Prairies exhibit more unusual trends.

How the Clusters of Maximum Temperature Change are Different between Clusters Across Canada

Figure 4.11 shows maximum temperature change trends across the 18 splits for 4 clusters, each panel representing the slope distribution for a different cluster.

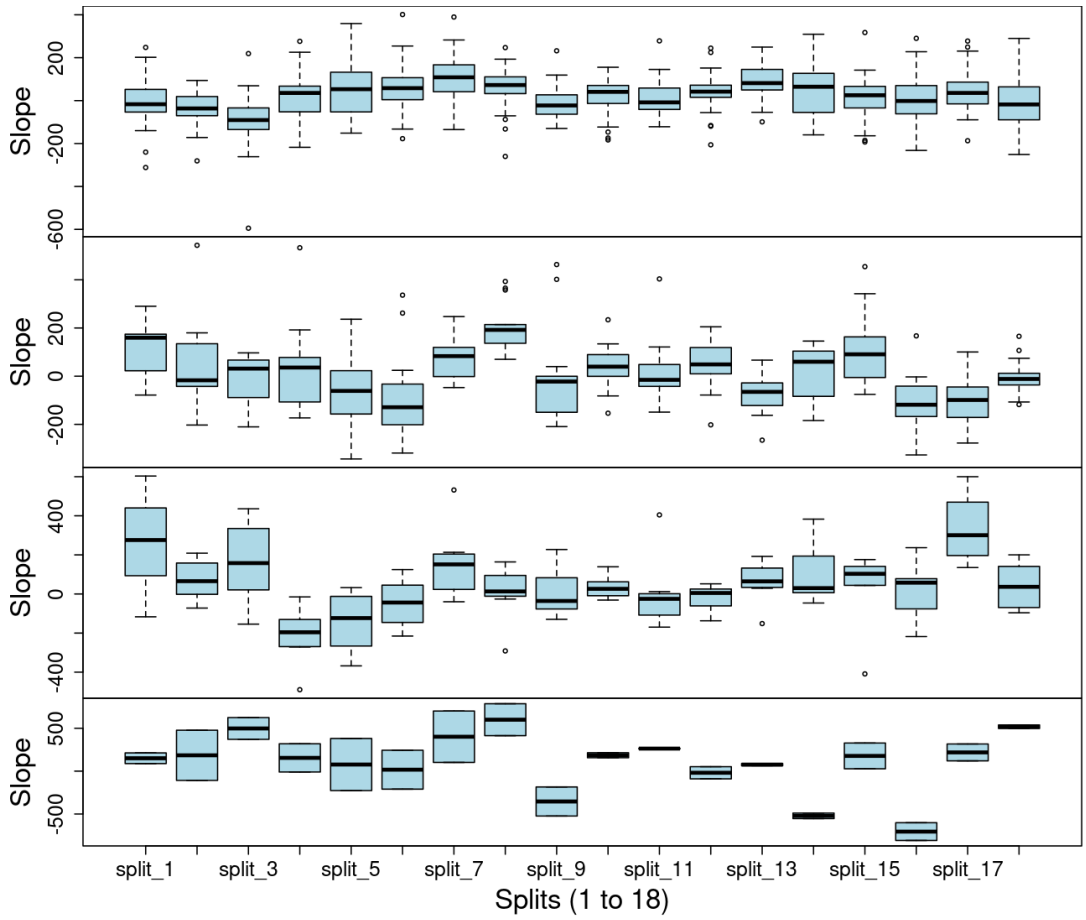

Figure 4.11: The distribution of the slope values of hourly maximum temperature changes across 18 splits for each of 4 clusters from the $k = 4$ realization of the clustering algorithm. Cluster 1 to Cluster 4 from top to bottom facets in this plot.

Similar to the cluster organization noticed in Figure 4.8, cluster 1 cuts across much of the country. Again, similar to what is observed in Figure 4.9, the slopes appear to be relatively stable across the splits but with the median slope of the temperature mainly hovering around zero. This suggests a minimal prolonged change in maximum temperature in these locations across the period of interest. Slight increases in some stations for some indexes are observed – i.e., index 8 is mostly positive, indicating higher maximums in the early summer.

Cluster 2 is similarly widely spread, from British Columbia to Quebec, and has

some very high variability. Maximums appear to be decreasing in the late winter and early spring, but then are much higher in late spring and early summer. The characteristic of this cluster is likely the indexes 5-8, with the steep decreases in maximums in indexes 5 and 6, and increases in 7 and 8.

Cluster 3 is mainly locations in the Northern region and West Central, with the characteristics being warmer maximums through the winter months, cooler maximums in the spring, and approximately even during the summer and early autumn.

And finally, cluster 4 is again the oddities, and isn't really interesting for examination, for the same reasons as the 90th percentile and 10th percentile cases.

4.2.7 Conclusion

Clustering, while not a perfect tool, allows us to determine commonalities between widely spread geographic stations and their temperature trends. As a tool for identifying patterns, it appears to be quite well suited to this kind of data. The combination of these findings, and those of the last chapter where the pipeline and trend estimation procedure were developed, give analysts new tools for understanding climate change on a local level, even across widely spread geographies.

4.3 Clustering Mortality and Morbidity Risks due to Air Pollution

Air pollutants are known to have impact on human health. The risks (measured associations between residual effective mortality and an air pollutant of interest) have been extensively studied by Dr. Hwashin Shin of Health Canada, and also by Dr. Wesley Burr of Trent University. In this section, we take some of these risks, previously modelled in a study that explored lags and parameter specifications for

the assessment of the effects of air pollution on human health.

The previous study specifically clustered the mortality and morbidity risks associated with fine particulate matter ($PM_{2.5}$) and ozone (O_3). We extracted from the study results the Generalized Additive Models that were run, incorporating both air pollutant concentrations and temperature as independent variables, focusing on lag 0 to capture immediate effects. Furthermore, the previous study included separate models for mortality and morbidity risks during cold seasons, hot seasons, and all seasons. We will examine the possible clusters of these risks across Canada. The features extracted from these models for clustering were:

- model estimates
- standard errors
- p-values

and these additional features were added to cluster spatial densities:

- latitude
- longitude.

In this section, we demonstrate how mortality and morbidity risks, derived from the cold, hot, and all-season models, cluster regionally across Canada. The clustering analysis employs the Density-Based Spatial Clustering of Applications with Noise (DBSCAN) algorithm, as described in Section 4.1.3. By utilizing DBSCAN, we aim to uncover spatial patterns and regional variations in health risks, providing insight into the influence of air pollution and temperature on public health outcomes across diverse climatic and geographical contexts in Canada. Recall that DBSCAN will automatically determine the "best" number of clusters to form in order to minimize the criterion, so unlike the previous slope work above, we will end with models that do not have a consistent number of clusters.

4.3.1 Clusters of Morbidity Risk in Different Seasons Across Canada due to $PM_{2.5}$

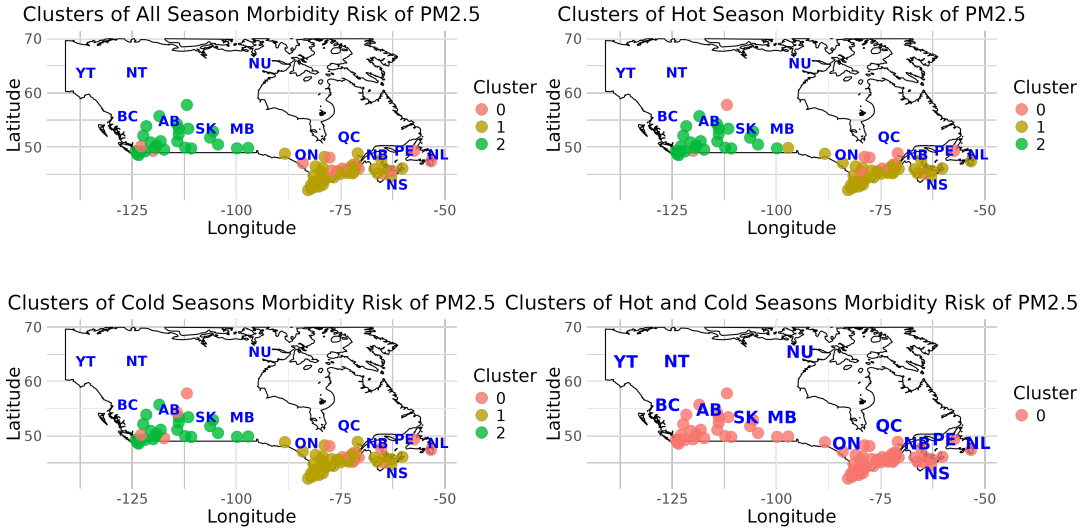

Figure 4.12: Canada with clusters of morbidity (hospitalization) risk due to $PM_{2.5}$ across different regions.

The clustering in Figure 4.12 suggests that the morbidity risks due to $PM_{2.5}$ ambient concentration vary significantly across Canada. Seasonally, the hot, cold, and all-season clustering maps display three distinct clusters, except for the combined hot-and-cold clustering map, which forms a single cluster. Additionally, the seasonal maps highlight a clear distinction in morbidity risk between two regional groups: the Prairies and Western Canada as one group, and West Central Canada and Atlantic Canada as another. Within these groups, the clusters show only minor variations, emphasizing regional similarities in morbidity risk patterns.

4.3.2 Clusters of Morbidity Risk in Different Seasons Across Canada due to O_3

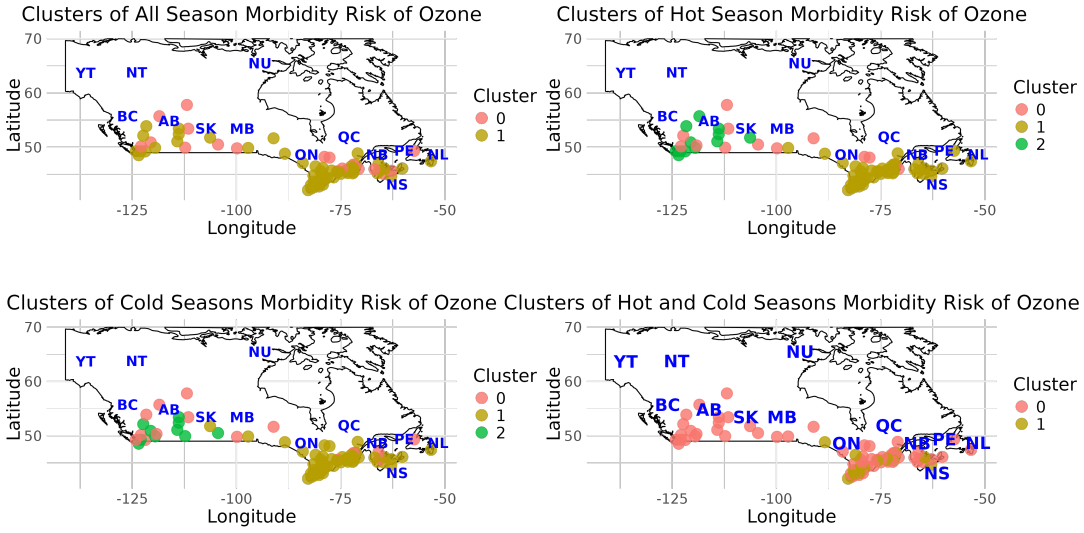

Figure 4.13: Canada with clusters of morbidity risk due to O_3 across different regions.

Compared to Figure 4.12, Figure 4.13 reveals a broader distribution of morbidity risk due to ozone exposure across different regions. For instance, the all-season map highlights notable similarities in morbidity risk from Atlantic Canada extending to the Western region, indicating a more widespread hospitalization risk across Canada linked to ozone deposition. The hot and cold season maps also display distinct variations in morbidity risk, similar to those observed for $PM_{2.5}$ in Figure 4.12, but with slightly greater diversity, particularly within the Prairies and Western region group.

4.3.3 Clusters of Mortality Risk in Different Seasons Across Canada due to $PM_{2.5}$

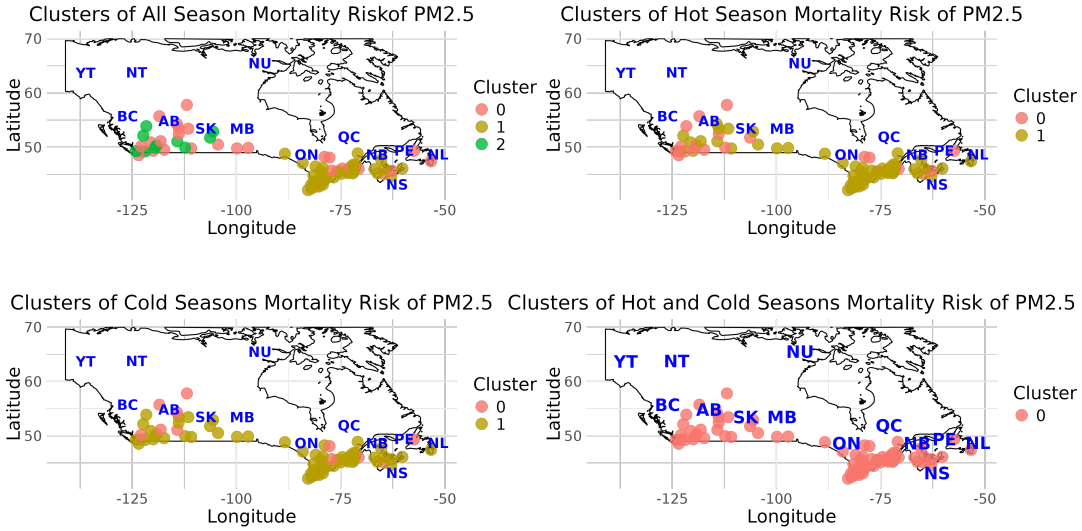

Figure 4.14: Canada with clusters of mortality risk due to $PM_{2.5}$ across different regions.

Similar to the clustering of morbidity risk due to $PM_{2.5}$ and O_3, mortality risk from these pollutants also exhibits distinct regional clusters across Canada. Figure 4.14 illustrates these clusters for different seasons and seasonal combinations (hot and cold). The all-season cluster displays greater variability and more distinct regional patterns compared to the hot and cold seasons. The individual hot and cold season clusters reveal relatively similar regional mortality risk patterns, spanning from Atlantic Canada to the Western region, with a few localized exceptions.

4.3.4 Clusters of Mortality Risk in Different Seasons Across Canada due to O_3

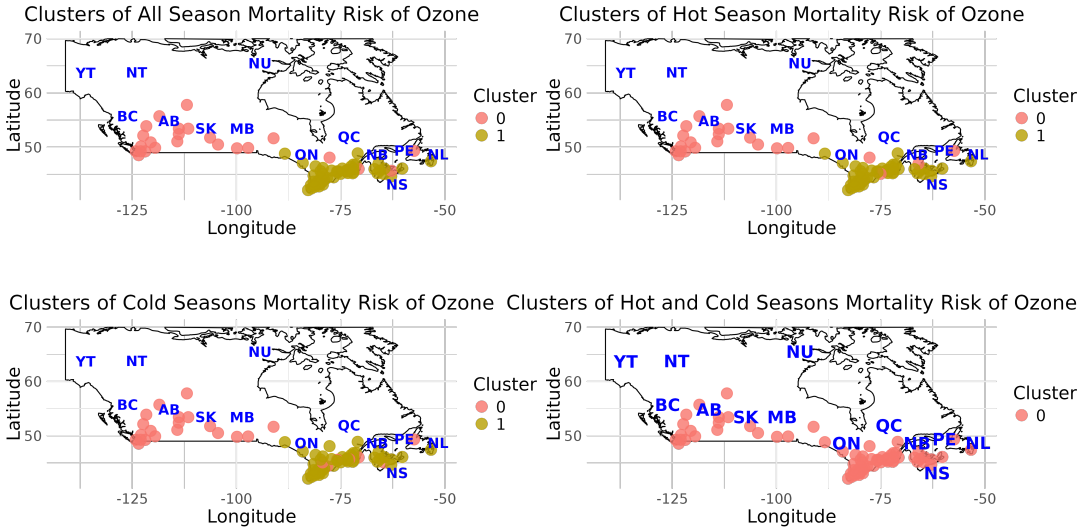

Figure 4.15: Canada with clusters of mortality risk due to O_3 across different regions (Region1 = BC=Western region, Region2 = Northern region, Region3 = Prairies = [AB, SK, MB], Region4 = West Central = [ON], Region5 = West Central = Quebec, Region6 = Atlantic = [NS, PE, NL]

Figure 4.15 shows two distinct clusters for each season, except for the combined hot and cold season. Each season with two clusters clearly highlights one group forming a cluster through the Prairies, the Western region, and northern Canada, while another group spans West-Central Canada and Atlantic Canada, forming the second cluster. A few exceptions exist where locations with mortality risk due to ozone in the first group (Western and Prairie regions) overlap with the second group (Central and Atlantic Canada).

4.3.5 Conclusion

This section was not intended to be a large contribution to the thesis, but simply to note that the techniques developed and examined for clustering of climate change trends can also be applied to risks, and in doing so, interesting comparisons can arise. For example, despite the clustering of all-season mortality risk due to O_3 largely splitting the country in two along east/west lines, some census division results on the east coast were clustered with the west coast, possibly indicating some moderation from climate effects – an excellent topic for future research.

5. *Conclusion*

This thesis has explored the application of Bayesian modeling and clustering techniques to assess climate change patterns in Canada, with a particular focus on temperature variability across multiple regions. Through the use of Bayesian hierarchical models and clustering algorithms, we aimed to enhance the understanding of how temperature-related climate variables are changing over time and across diverse geographical regions in Canada. The innovative pipeline developed, which takes hourly observations at disparate climate stations and integrates them across multiple hierarchical levels, concluding with Bayesian modelling and clustering, appears to have provided a useful tool for underestanding climate change in Canada, and its realization on a number of local scales.

The study utilized hourly temperature data from multiple climate stations across Canada, split into 18 temporal indexed parts, to capture the detailed fluctuations and trends within these regions over an extended (30 year) period. By first splitting the data and calculating key metrics such as mean, minimum, maximum, and percentile temperatures, we were able to generate more granular insights into the temporal shifts in temperature on a local scale. The Bayesian modeling framework, both at the national and regional levels, allowed us to pool our understanding of temperature changes with every new data point, while accounting for uncertainties inherent in the data.

One of the significant contributions of this thesis is the combination of the pipeline

for local temporal trends in climate and the application of Bayesian hierarchical models to estimate national and regional temperature changes. The single-level models provided a national perspective, while the two-level models incorporated regional influences, demonstrating how different parts of Canada have experienced distinct temperature patterns. The findings showed that while some regions, like the Northern and Prairie regions, experienced more extreme changes, other regions, such as British Columbia, exhibited complex multi-modal temperature distributions due to unique geographical and topographical factors. This regional analysis underscores the importance of localized climate studies, as national averages may obscure critical regional variations in temperature trends.

Furthermore, the clustering analysis, which segmented Canada into various regions based on temperature trends and variability, provided valuable insights into regional climate behavior. The application of hierarchical clustering, combined with feature-based analysis of temperature data, allowed us to classify regions with similar temperature change patterns. For example, the clustering of average temperatures revealed strong correlations between certain regions, such as the Prairies and West Central Canada, where similar temperature patterns emerged despite geographic separation. The clustering of extremes, such as the 10th and 90th percentiles of temperature, revealed regions experiencing the most significant fluctuations, with important implications for understanding climate risk and resilience across Canada.

One of the key insights from this study is the observation of increased temperature variability in regions like British Columbia, where complex topographical factors contribute to unique temperature distributions. The findings align with existing literature that highlights the intricacies of temperature changes in regions with varied elevations and microclimate. Additionally, the Northern regions exhibited notable warming trends, particularly during traditionally colder months, suggesting that climate change is having a profound impact on the Arctic and sub-Arctic areas of

Canada.

We were also able to apply the same approach, clustering across disparate geography, to demonstrate the potential of clustering as a tool for understanding similarities in risks due to air pollution exposure. The patterns observed highlight the need for region-specific and season-specific risk management strategies, tailored to address both pollutant types and associated health outcomes effectively.

In conclusion, this thesis contributes to the growing body of research on climate change by providing a detailed analysis of temperature variability in Canada using time series methods, Bayesian modeling and clustering methods. The findings have significant implications for understanding the spatial and temporal dynamics of climate change in Canada, and they highlight the need for localized climate strategies that take into account regional differences in climate behavior. The study demonstrates the power of combining time series mesthods, Bayesian inference and clustering analysis to uncover hidden patterns in locally- or regionally-centred climate data, providing a robust framework that can be applied to other climate variables in future research.

Looking forward, there are several potential avenues for future work. First, expanding the analysis to include other essential climate variables, such as precipitation, wind speed, and humidity, would provide a more holistic view of climate change impacts in Canada. Additionally, the integration of more sophisticated covariates, such as land use changes, urbanization patterns, or greenhouse gas emissions into the Bayesian models could further enhance the predictive power of the analysis. Furthermore, the development of real-time climate monitoring systems based on Bayesian models could provide policymakers with up-to-date probabilistic forecasts of climate trends, enabling more effective climate adaptation and mitigation efforts. Finally, clustering based on the magnitude of mortality and morbidity risk can be performed to identify which regions are more at risk and which are less at risk having considered

the climate variability and pollutants deposition.

The results of this thesis offer a solid foundation for future studies and contribute to the ongoing effort to better understand and respond to the complex challenges posed by climate change in Canada. The insights gained from this research not only deepen our understanding of how climate variables are changing, but also offer practical tools for guiding decision-makers as they address the impacts of climate change on communities, ecosystems, and economies.

Bibliography

[1] S. Aghabozorgi, A.S. Shirkhorshidi, and T.Y. Wah. Time-series clustering – a decade review. *Information Systems*, 53:16–38, 2015.

[2] S. Arrhenius. On the influence of carbonic acid in the air upon the temperature of the earth. *Philosophical Magazine*, 41:237–276, 1896.

[3] C. Augustin, B. Bertrand, V. Robert, S. Sophie, R.S Trivikrama, S. Simone, K. Zbigniew, L. Menut, C. Gaëlle, M. Frederik, and R. Laurence. European atmosphere in 2050, a regional air quality and climate perspective under CMIP5 scenarios. *Atmospheric Chemistry and Physics*, 13:6455–6499, 2013.

[4] G. Bal, E. Rivot, J. Baglinière, J. White, and E. Prévost. A hierarchical Bayesian model to quantify uncertainty of stream water temperature forecasts. *PLoS One*, 9(12):e115659, 2014.

[5] S. Bojinski, M. Verstraete, T.C. Peterson, C. Richter, A. Simmons, and M. Zemp. The concept of essential climate variables in support of climate research, applications, and policy. *Bulletin of the American Meteorological Society*, 95(9):1431–1443, 2014.

[6] B.R. Bonsal, X. Zhang, L.A. Vincent, and W.D. Hogg. Characteristics of daily and extreme temperatures over Canada. *Journal of Climate*, 14(9):1959–1976, 2001.

[7] M. Bottomley, C.K. Folland, J. Hsiung, R.E. Newell, and D.E. Parker. *Global Ocean Surface Temperature Atlas (GOSTA)*. HMSO, London, 1990. Joint UK

Met. Office/Massachussetts Institute of Technology Project.

[8] S. Brönnimann. *Climatic Changes Since 1700*. Advances in Global Change Research. Springer International Publishing, Cham, 1st edn. edition, 2015.

[9] S. Brönnimann, R. Allan, L. Ashcroft, S. Baer, M. Barriendos, R. Brázdil, Y. Brugnara, M. Brunet, M. Brunetti, B. Chimani, et al. Unlocking pre-1850 instrumental meteorological records: A global inventory. *Bulletin of the American Meteorological Society*, 100(12):ES389–ES413, 2019.

[10] A. Burgdorf. A global inventory of quantitative documentary evidence related to climate since the 15th century. *Climate of the Past*, 18(6):1407–1428, 2022.

[11] R. Campello, P. Kröger, J. Sander, and A. Zimek. Density-based clustering. *Wiley Interdisciplinary Reviews: Data Mining and Knowledge Discovery*, 10(2):e1343, 2020.

[12] P.C. Cheeseman, J.C. Stutz, et al. Bayesian classification (autoclass): theory and results. *Advances in knowledge discovery and data mining*, 180:153–180, 1996.

[13] G.P. Compo, J.S. Whitaker, P.D. Sardeshmukh, N. Matsui, R.J. Allan, X. Yin, B.E. Gleason Jr, R.S. Vose, G. Rutledge, P. Bessemoulin, et al. Review article the twentieth century reanalysis project. 2011.

[14] N.S. Diffenbaugh and F. Giorgi. Climate change hotspots in the CMIP5 global climate model ensemble. *Climatic Change*, 114:813–822, 2012.

[15] F.W. Dobson. Oceanic changes associated with global increases in atmospheric carbon dioxide: A preliminary report for the Atlantic Coast of Canada. 1986.

[16] D.B. Dunson. Commentary: practical advantages of Bayesian analysis of epidemiologic data. *American Journal of Epidemiology*, 153(12):1222–1226, 2001.

[17] P. Eckle and P. Burgherr. Bayesian data analysis of severe fatal accident risk in the oil chain. *Risk Analysis: An International Journal*, 33(1):146–160, 2013.

[18] P.N. Edwards. History of climate modeling. *Wiley Interdisciplinary Reviews:*

Climate Change, 2(1):128–139, 2011.

[19] H.W. Ellsaesser et al. On the radiative and dynamical influences of cloud changes associated with climatic warming. *Reviews of Geophysics*, 24(4):745–755, 1986.

[20] M.T.M. Espinosa, G. Giuliani, and N. Ray. Reviewing the discoverability and accessibility to data and information products linked to Essential Climate Variables. *International Journal of Digital Earth*, 2019.

[21] J.B. Fourier. M'emoire sur les temp'eratures du globe terrestre et des espaces plan'etaires. *M'emoires de l'Acad'emie des Sciences de l'Institut de France*, 7:569–604, 1827.

[22] A. Gelman, J.B. Carlin, H.S. Stern, and D.B. Rubin. *Bayesian Data Analysis*. Chapman and Hall/CRC, 1995.

[23] A. Gelman and D.B. Rubin. Inference from iterative simulation using multiple sequences. *Statistical science*, 7(4):457–472, 1992.

[24] E Halley. An historical account of the trade winds and monsoons observable in the seas between and near the tropics with an attempt to assign a physical cause of the said winds. *Phil. Trans. R. Society, London*, pages 153–68, 1753.

[25] J. Han, J. Pei, and H. Tong. *Data mining: concepts and techniques*. Morgan kaufmann, 2022.

[26] J. Hansen, M. Sato, J. Glascoe, and R. Ruedy. A common-sense climate index: Is climate changing noticeably? *Proceedings of the National Academy of Sciences*, 95(8):4113–4120, 1998.

[27] Z. Hao, A. AghaKouchak, and T.J Phillips. Changes in concurrent monthly precipitation and temperature extremes. *Environmental Research Letters*, 8(3):034014, 2013.

[28] M.R. Haylock, G.C. Cawley, C. Harpham, R.L. Wilby, and C.M. Goodess. Downscaling heavy precipitation over the United Kingdom: a comparison of dynamical and statistical methods and their future scenarios. *International Journal of*

Climatology: A Journal of the Royal Meteorological Society, 26(10):1397–1415, 2006.

[29] G.C. Hegerl, S. Brönnimann, T Cowan, A.R. Friedman, E Hawkins, C. Iles, W Müller, A. Schurer, and S. Sabine Undorf. Causes of climate change over the historical record. *Environmental Research Letters*, 14(12):123006, dec 2019.

[30] C. Hellström, D. Chen, C. Achberger, and J. Räisänen. Comparison of climate change scenarios for Sweden based on statistical and dynamical downscaling of monthly precipitation. *Climate Research*, 19(1):45–55, 2001.

[31] F. Hourdin, M.A. Foujols, F. Codron, V. Guemas, J.L. Dufresne, S. Bony, S. Denvil, L. Guez, F. Lott, J. Ghattas, P. Braconnot, O. Marti, Y. Meurdesoif, and L. Bopp. Impact of the LMDZ atmospheric grid configuration on the climate and sensitivity of the IPSL-CM5A coupled model. *Climate Dynamics*, 40:2167–2192, 2012.

[32] M. Hulme and P.D Jones. Global climate change in the instrumental period. *Environmental Pollution*, 83(1):23–36, 1994.

[33] K.T. Jessica and J. R. Gyakum. Trends in Canadian surface temperature variability in the context of climate change. *Atmosphere-Ocean*, 48(3):147–162, 2010.

[34] X. Jiang and Z. Yang. Projected changes of temperature and precipitation in Texas from downscaled global climate models. *Climate Research*, 53(3):229–244, 2012.

[35] P. D. Jones and R.S. Bradley. Climate since the commencement of instrumental records. In R. S. Bradley and P. D. Jones, editors, *Climate since A.D. 1500*, pages 246–268. Routledge, London, 1992.

[36] P. D. Jones and K. Briffa. Global surface air temperature variations: Part i the instrumental period. *Holocene*, 2:174–188, 1992.

[37] P. D. Jones and T. M. L. Wigley. Satellite data under scrutiny. *Nature*, 344:711, 1990.

[38] P.D. Jones, D.H. Lister, T.J. Osborn, C. Harpham, M. Salmon, and C.P. Morice. Hemispheric and large-scale land-surface air temperature variations: An extensive revision and an update to 2010. *Journal of Geophysical Research: Atmospheres*, 117(D5), 2012.

[39] P.D. Jones, T.M.L. Wigley, and P.B. Wright. Global temperature variations between 1861 and 1984. *Nature*, 322:430–434, 1986.

[40] T.R. Karl and P.D. Jones. Urban bias in area-averaged surface air temperature trends. *Bulletin of the American Meteorological Society*, 70:265–270, 1989.

[41] D.J. Karoly and K. Braganza. Identifying global climate change using simple indices. *Geophysical Research Letters*, 28(11):2205–2208, 2001.

[42] M. Katzfuss, D. Hammerling, and R.L. Smith. A Bayesian hierarchical model for climate change detection and attribution. *Geophysical Research Letters*, 44(11):5720–5728, 2017.

[43] L. Kaufman and P.J. Rousseeuw. *Finding groups in data: an introduction to cluster analysis*. John Wiley & Sons, 2009.

[44] J.J. Kennedy, C.P. Morice, D.E. Parker, and H. Titchner. Global and regional climate in 2012. *Weather (00431656)*, 68(9), 2013.

[45] P. Laloyaux, E. de Boisseson, M. Balmaseda, J. Bidlot, S. Broennimann, R. Buizza, P. Dalhgren, D. Dee, L. Haimberger, and H. Hersbach. CERA-20C: a coupled reanalysis of the twentieth century. *Journal of Advances in Modeling Earth Systems*, 10(5):1172–1195, 2018.

[46] T.W. Liao. Clustering of time series data—a survey. *Pattern recognition*, 38(11):1857–1874, 2005.

[47] Z. Liu, M. Cheng, Z. Li, Z. Huang, Q. Liu, Y. Xie, and E. Chen. Adaptive normalization for non-stationary time series forecasting: A temporal slice perspective. *Advances in Neural Information Processing Systems*, 36, 2024.

[48] S.M. Lynch. *Introduction to applied Bayesian statistics and estimation for social*

scientists, volume 1. Springer, 2007.

[49] J. Macqueen. Some methods for classification and analysis of multivariate observations. In *Proceedings of 5th Berkeley Symposium on Mathematical Statistics and Probability/University of California Press*, 1967.

[50] C.A. Matthew. Historical Background. In *Eratosthenes and the Measurement of the Earth's Circumference (c.230 BC)*. Oxford University Press, 06 2023.

[51] E.P. Maurer. Uncertainty in hydrologic impacts of climate change in the Sierra Nevada Mountains, California under two emissions scenarios. *Climatic Change*, 82:309–325, 2007.

[52] P.D. McNicholas. *Mixture model-based classification*. CRC Press, 2016.

[53] K. Morgan. Data mining: Concepts and techniques. *Mining, What Is Data*, 10(559-569):4, 2006.

[54] R.A. Muller, J. Curry, D. Groom, R. Jacobsen, S. Perlmutter, R. Rohde, A. Rosenfeld, C. Wickham, and J. Wurtele. Decadal variations in the global atmospheric land temperatures. *Journal of Geophysical Research: Atmospheres*, 118(11):5280–5286, 2013.

[55] L.A. Mysak and C.A. Lin. Role of the oceans in climatic variability and climatic change. *Canadian Geographer/Le Géographe canadien*, 34(4):352–369, 1990.

[56] K. Müller, H. Wickham, David A.J., and Falcon. S. *RSQLite: SQLite Interface for R*, 2024. R package version 2.3.7.

[57] L. Naitza, P. Cristofanelli, A. Marinoni, F. Calzolari, F. Roccato, Maurizio Busetto, Damiano Sferlazzo, Eleonora Aruffo, Piero Di Carlo, Mariantonia Bencardino, et al. Increasing the maturity of measurements of essential climate variables (ECVs) at Italian atmospheric WMO/GAW observatories by implementing automated data elaboration chains. *Computers & Geosciences*, 137:104432, 2020.

[58] NOAA National Centers for Environmental Information. Annual 2023 Global Climate Report. `https://www.ncei.noaa.gov/access/monitoring/`

monthly-report/global/202313/, 2024. Accessed: 2024-01-17.

[59] A.H. Oort et al. The impact of the warm equatorial ocean on the atmosphere. *Climate Dynamics*, 2(1):29–46, 1987.

[60] S. M. Papalexiou, A. AghaKouchak, K.E. Trenberth, and E. Foufoula-Georgiou. Global, regional, and megacity trends in the highest temperature of the year: Diagnostics and evidence for accelerating trends. *Earth's Future*, 6(1):71–79, 2018.

[61] J.M. Pfadt, D.V.D. Bergh, K. Sijtsma, and E.J. Wagenmakers. A tutorial on Bayesian single-test reliability analysis with JASP. *Behavior Research Methods*, 55(3):1069–1078, 2023.

[62] D.W. Pierce, T. Das, D.R. Cayan, E.P. Maurer, N.L. Miller, Y. Bao, M. Kanamitsu, K. Yoshimura, M.A. Snyder, L.C. Sloan, et al. Probabilistic estimates of future changes in California temperature and precipitation using statistical and dynamical downscaling. *Climate Dynamics*, 40:839–856, 2013.

[63] P. Poli, H. Hersbach, D.P. Dee, P. Berrisford, A.J. Simmons, F. Vitart, P. Laloyaux, D. Tan, C. Peubey, J. Thépaut, et al. ERA-20C: An atmospheric reanalysis of the twentieth century. *Journal of Climate*, 29(11):4083–4097, 2016.

[64] P. Rai, S. Singh, et al. A survey of clustering techniques. *International Journal of Computer Applications*, 7(12):1–5, 2010.

[65] V. Ramanathan. The greenhouse theory of climate change: a test by an inadvertent global experiment. *Science*, 240(4850):293–299, 1988.

[66] D.M. Romps. Heat index extremes increasing several times faster than the air temperature. *Environmental Research Letters*, 19(4):041002, 2024.

[67] J. Schmidli, C.M. Goodess, C. Frei, M.R. Haylock, Y. Hundecha, J. Ribalaygua, and T. Schmith. Statistical and dynamical downscaling of precipitation: An evaluation and comparison of scenarios for the European Alps. *Journal of Geophysical Research: Atmospheres*, 112(D4), 2007.

[68] R.L. Smith, C. Tebaldi, D. Nychka, and L.O. Mearns. Bayesian modeling of uncertainty in ensembles of climate models. *Journal of the American Statistical Association*, 104(485):97–116, 2009.

[69] T. Spence and J. Townshend. The Global Climate Observing System (GCOS): An Editorial. In *Long-Term Climate Monitoring by the Global Climate Observing System: International Meeting of Experts*, pages 1–4. Springer, 1996.

[70] K. Stahl, R.D. Moore, J.A. Floyer, M.G. Asplin, and I.G. McKendry. Comparison of approaches for spatial interpolation of daily air temperature in a large region with complex topography and highly variable station density. *Agricultural and Forest Meteorology*, 139(3-4):224–236, 2006.

[71] Stan Development Team. *Stan User's Guide*, 2024. Available at `https://mc-stan.org/docs/stan-users-guide/index.html`.

[72] C. Tebaldi, L.O. Mearns, D. Nychka, and R.L. Smith. Regional probabilities of precipitation change: A Bayesian analysis of multimodel simulations. *Geophysical Research Letters*, 31(24), 2004.

[73] C. Tebaldi and B. Sansó. Joint projections of temperature and precipitation change from multiple climate models: a hierarchical bayesian approach. *Journal of the Royal Statistical Society Series A: Statistics in Society*, 172(1):83–106, 2009.

[74] C. Tebaldi, R.L. Smith, D. Nychka, and L.O. Mearns. Quantifying uncertainty in projections of regional climate change: A Bayesian approach to the analysis of multimodel ensembles. *Journal of Climate*, 18(10):1524–1540, 2005.

[75] M. Turco, E. Palazzi, J. Von-Hardenberg, and A. Provenzale. Observed climate change hotspots. *Geophysical Research Letters*, 42(9):3521–3528, 2015.

[76] P.D. Tyson. *Climatic Change and Variability in Southern Africa*. Oxford University Press, Cape Town, 1986.

[77] J. Uppenbrink. Arrhenius and global warming. *Science*, 272(5265):1122–1122,

1996.

[78] L. A. Vincent, X. Zhang, R. D. Brown, Y. Feng, E. Mekis, E. J. Milewska, H. Wan, and X. L. Wang. Observed trends in Canada's climate and influence of low-frequency variability modes. *Journal of Climate*, 28(11):4545 – 4560, 2015.

[79] L.A. Vincent. A technique for the identification of inhomogeneities in Canadian temperature series. *Journal of Climate*, 11(5):1094–1104, 1998.

[80] L.A. Vincent and D.W. Gullett. Canadian historical and homogeneous temperature datasets for climate change analyses. *International Journal of Climatology: A Journal of the Royal Meteorological Society*, 19(12):1375–1388, 1999.

[81] L.A. Vincent, M.M. Hartwell, and X.L. Wang. A third generation of homogenized temperature for trend analysis and monitoring changes in Canada's climate. *Atmosphere-Ocean*, 58(3):173–191, 2020.

[82] L.A. Vincent, X. Zhang, B.R. Bonsal, and W.D. Hogg. Homogenized daily temperatures for trend analysis in extremes over Canada. In *Preprints, 12th Conference on Applied Climatology*, pages 86–89. American Meteorological Society Asheville, NC, 2000.

[83] L.A. Vincent, X. Zhang, R.D. Brown, Y. Feng, E. Mekis, E.J. Milewska, H. Wan, and X.L. Wang. Observed trends in Canada's climate and influence of low-frequency variability modes. *Journal of Climate*, 28(11):4545 – 4560, 2015.

[84] W. Wang, J. Yang, R. Muntz, et al. STING: a statistical information grid approach to spatial data mining. In *Proceedings of Very Large Databases (VLDB)*, volume 97, pages 186–195, 1997.

[85] Richard W.K. Statistical procedures for making inferences about climate variability. *Journal of Climate*, 1(11):1057 – 1064, 1988.

[86] A.W. Wood, L.R. Leung, V. Sridhar, and D.P. Lettenmaier. Hydrologic implications of dynamical and statistical approaches to downscaling climate model outputs. *Climatic Change*, 62:189–216, 2004.

[87] B. Wu and B.M. Wilamowski. A fast density and grid based clustering method for data with arbitrary shapes and noise. *IEEE Transactions on Industrial Informatics*, 13(4):1620–1628, 2016.

[88] Z. Yu, F. Montalto, S. Jacobson, U. Lall, D. Bader, and R. Horton. Stochastic downscaling of hourly precipitation series from climate change projections. *Water Resources Research*, 58(10):e2022WR033140, 2022.

[89] X. Zhang, L.A. Vincent, W.D. Hogg, and A. Niitsoo. Temperature and precipitation trends in Canada during the 20th century. *Atmosphere-Ocean*, 38(3):395–429, 2000.

A. *Diagnostics for Stan Model Fits*

The following tables are the full output diagnostics from the one- and two-level hierarchical Bayesian models used to estimate the national temperature trends.

Parameter	Rhat	n_eff	mean	sd	2.5%	50%	97.5%
mu	1.1	96	-2.4	4.3	-10.3	-2.7	6.4
Sigma	1.1	47	4.8	4.1	1.1	3.3	16.4
stationbeta[1]	1.0	266	-3.2	7.4	-18.6	-3.2	11.3
stationbeta[2]	1.0	263	-1.8	7.5	-15.2	-2.2	14.5
stationbeta[3]	1.0	279	-2.5	7.5	-18.4	-2.9	13.3
stationbeta[4]	1.0	293	-3.4	7.5	-19.8	-3.3	11.0
stationbeta[5]	1.0	273	-3.2	7.3	-19.2	-3.4	11.6
stationbeta[6]	1.0	291	-1.9	7.9	-16.1	-2.4	16.0
stationbeta[7]	1.0	296	-2.2	7.7	-17.5	-2.7	14.8
stationbeta[8]	1.0	288	-2.7	7.6	-17.6	-3.0	13.6
stationbeta[9]	1.0	276	-2.3	7.5	-16.7	-2.8	14.3
stationbeta[10]	1.0	330	-2.5	7.9	-18.0	-2.8	13.8

Parameter	Rhat	n_eff	mean	sd	2.5%	50%	97.5%
stationbeta[11]	1.0	314	-2.6	7.4	-18.2	-2.8	12.6
stationbeta[12]	1.0	272	-1.8	7.6	-16.4	-2.4	15.6
stationbeta[13]	1.0	287	-2.4	7.4	-16.7	-2.7	13.7
stationbeta[14]	1.0	291	-2.1	7.7	-16.7	-2.6	15.4
stationbeta[15]	1.0	287	-2.6	7.5	-17.9	-2.9	12.5
stationbeta[16]	1.0	286	-2.6	7.5	-17.2	-2.9	12.9
stationbeta[17]	1.0	317	-2.5	7.8	-18.0	-2.8	15.2
stationbeta[18]	1.0	280	-2.3	7.3	-16.4	-2.6	13.5
stationbeta[19]	1.0	312	-2.2	7.8	-17.0	-2.5	15.1
stationbeta[20]	1.0	292	-2.4	7.5	-16.8	-2.9	14.1
stationbeta[21]	1.0	332	-2.6	7.8	-17.7	-2.9	14.4
stationbeta[22]	1.0	316	-2.4	7.6	-17.1	-2.8	13.2
stationbeta[23]	1.0	284	-2.4	7.6	-16.6	-2.8	13.7
stationbeta[24]	1.0	268	-2.0	7.4	-16.2	-2.5	14.0
stationbeta[25]	1.0	330	-2.4	7.7	-18.5	-2.6	13.9
stationbeta[26]	1.0	281	-2.3	7.4	-16.3	-2.8	14.2
stationbeta[27]	1.0	276	-2.6	7.2	-17.6	-2.8	12.0
stationbeta[28]	1.0	310	-2.4	7.6	-16.6	-2.7	13.8
stationbeta[29]	1.0	316	-2.4	7.8	-17.8	-2.7	14.0
stationbeta[30]	1.0	339	-2.2	7.8	-16.8	-2.6	14.0
stationbeta[31]	1.0	262	-2.0	7.5	-16.3	-2.5	15.0
stationbeta[32]	1.0	296	-2.5	7.5	-16.5	-2.9	12.9
stationbeta[33]	1.0	321	-2.5	7.7	-17.8	-2.8	13.4
stationbeta[34]	1.0	252	-1.8	7.7	-14.9	-2.6	15.9

Parameter	Rhat	n_eff	mean	sd	2.5%	50%	97.5%
stationbeta[35]	1.0	326	-2.5	7.7	-17.6	-2.8	14.4
stationbeta[36]	1.0	282	-2.6	7.7	-18.0	-2.9	13.2
stationbeta[37]	1.0	300	-2.7	7.5	-17.7	-2.9	13.0
stationbeta[38]	1.0	268	-1.9	7.6	-16.3	-2.4	15.2
stationbeta[39]	1.0	297	-2.8	7.6	-18.5	-2.9	12.6
stationbeta[40]	1.0	285	-2.7	7.4	-18.7	-2.8	12.1
stationbeta[41]	1.0	286	-2.4	7.5	-17.3	-2.7	14.2
stationbeta[42]	1.0	341	-2.5	7.9	-17.8	-2.8	14.7
stationbeta[43]	1.0	299	-2.5	7.6	-17.5	-2.8	13.6
stationbeta[44]	1.0	305	-2.7	7.3	-17.8	-2.9	13.1
stationbeta[45]	1.0	310	-2.1	7.7	-15.9	-2.4	14.9
stationbeta[46]	1.0	279	-2.6	7.3	-17.5	-2.8	13.1
stationbeta[47]	1.0	267	-2.2	7.3	-16.1	-2.5	13.9
stationbeta[48]	1.0	282	-2.2	7.3	-16.9	-2.6	14.2
stationbeta[49]	1.0	303	-2.7	7.4	-18.1	-2.8	12.9
stationbeta[50]	1.0	285	-2.6	7.3	-17.0	-2.8	12.8
stationbeta[51]	1.0	285	-2.4	7.3	-16.9	-2.7	12.4
stationbeta[52]	1.0	292	-2.5	7.7	-17.8	-2.7	13.8
stationbeta[53]	1.0	326	-2.5	7.8	-17.2	-2.7	13.6
stationbeta[54]	1.0	304	-2.5	7.7	-17.1	-3.0	13.9
stationbeta[55]	1.0	303	-2.6	7.4	-17.1	-2.9	12.3
stationbeta[56]	1.0	287	-2.6	7.4	-17.5	-2.9	12.9

Parameter	Rhat	n_eff	mean	sd	2.5%	50%	97.5%
stationbeta[57]	1.0	339	-2.5	7.7	-18.1	-2.8	13.1
stationbeta[58]	1.0	318	-2.5	7.7	-17.2	-2.7	13.1
stationbeta[59]	1.0	289	-2.6	7.2	-16.6	-2.7	12.1
stationbeta[60]	1.0	267	-2.1	7.5	-17.1	-2.6	14.0
stationbeta[61]	1.0	248	-1.8	7.6	-15.6	-2.4	14.9

Table A.1: Diagnostics for the Bayesian Level 1 Model for Average Temperature.

Parameter	Rhat	n_eff	mean	sd	2.5%	50%	97.5%
mu	1.0	118	-1.3	4.7	-11.6	-1.1	7.3
SigmaC	1.1	31	4.5	3.5	1.3	3.4	12.9
SigmaR	1.0	68	5.3	6.9	0.4	2.6	25.7
stationbeta[1]	1.0	218	-3.5	10.2	-26.8	-2.4	13.7
stationbeta[2]	1.0	191	-2.7	9.9	-25.0	-1.6	14.3
stationbeta[3]	1.0	190	-3.0	10.1	-25.4	-1.8	14.3
stationbeta[4]	1.0	184	-3.8	9.9	-26.5	-2.7	12.7
stationbeta[5]	1.0	192	-3.5	9.7	-25.7	-2.4	12.6
stationbeta[6]	1.0	194	-2.8	9.8	-25.0	-1.7	14.4
stationbeta[7]	1.0	196	-2.8	9.9	-24.3	-2.1	14.5
stationbeta[8]	1.0	207	-3.2	9.9	-26.1	-2.4	14.6
stationbeta[9]	1.0	207	-3.2	10.0	-25.9	-2.2	14.3
stationbeta[10]	1.0	209	-2.7	9.8	-24.9	-1.4	14.7
stationbeta[11]	1.0	247	-1.1	10.4	-22.0	-0.8	20.0
stationbeta[12]	1.0	278	-0.4	10.5	-21.2	-0.6	19.8
stationbeta[13]	1.0	252	-0.8	10.3	-21.9	-0.5	19.9
stationbeta[14]	1.0	294	-0.6	10.4	-22.1	-0.5	19.6
stationbeta[15]	1.0	253	-2.6	10.5	-26.4	-1.9	16.4
stationbeta[16]	1.0	245	-2.8	10.4	-25.8	-2.1	16.6
stationbeta[17]	1.0	222	-3.0	10.9	-25.9	-2.0	16.3
stationbeta[18]	1.0	231	-2.3	10.3	-26.4	-1.4	17.3
stationbeta[19]	1.0	232	-2.2	10.4	-24.8	-1.5	16.8
stationbeta[20]	1.0	250	-2.6	10.6	-26.1	-2.0	16.9
stationbeta[21]	1.0	247	-2.6	10.2	-25.5	-1.9	17.0

Parameter	Rhat	n_eff	mean	sd	2.5%	50%	97.5%
stationbeta[22]	1.0	309	0.3	10.4	-18.5	-0.3	23.0
stationbeta[23]	1.0	319	0.4	10.8	-19.4	-0.2	23.9
stationbeta[24]	1.0	326	0.8	10.6	-18.1	0.1	24.8
stationbeta[25]	1.0	294	0.3	10.9	-20.2	-0.3	23.5
stationbeta[26]	1.0	337	0.6	10.9	-19.5	-0.1	24.4
stationbeta[27]	1.0	318	0.3	10.7	-19.1	-0.4	23.1
stationbeta[28]	1.0	336	0.5	10.5	-17.9	-0.4	23.4
stationbeta[29]	1.0	320	0.4	10.5	-17.8	-0.3	23.5
stationbeta[30]	1.0	313	0.5	10.4	-18.2	-0.4	23.3
stationbeta[31]	1.0	302	0.8	10.5	-18.4	-0.1	24.3
stationbeta[32]	1.0	319	0.3	10.7	-19.1	-0.4	23.3
stationbeta[33]	1.0	213	-0.0	11.0	-21.4	-0.6	22.8
stationbeta[34]	1.0	330	1.1	10.5	-18.0	0.4	24.0
stationbeta[35]	1.0	114	-4.6	11.1	-31.5	-2.9	13.1
stationbeta[36]	1.0	112	-4.4	11.2	-31.8	-2.6	13.0
stationbeta[37]	1.0	118	-4.5	11.3	-32.1	-2.6	11.9
stationbeta[38]	1.0	109	-4.3	11.4	-31.1	-2.6	14.2
stationbeta[39]	1.0	110	-4.5	11.0	-31.2	-2.8	13.0
stationbeta[40]	1.0	117	-4.8	11.2	-31.3	-2.9	13.0
stationbeta[41]	1.0	110	-4.4	11.1	-30.8	-2.6	13.5
stationbeta[42]	1.0	118	-4.5	11.2	-31.5	-3.0	13.3
stationbeta[43]	1.0	125	-4.5	11.8	-31.4	-2.9	13.4
stationbeta[44]	1.0	113	-4.3	11.1	-32.0	-2.4	13.1
stationbeta[45]	1.0	115	-4.3	11.1	-31.2	-2.7	13.1

Parameter	Rhat	n_eff	mean	sd	2.5%	50%	97.5%
stationbeta[46]	1.0	112	-4.4	11.1	-30.8	-2.6	13.6
statiostationa[47]	1.0	116	-4.2	11.0	-30.9	-2.5	13.4
stationbeta[48]	1.0	110	-4.4	11.0	-31.0	-3.0	13.6
stationbeta[49]	1.0	114	-4.6	11.2	-31.5	-2.9	13.1
stationbeta[50]	1.0	111	-4.6	11.1	-31.1	-2.8	13.2
stationbeta[51]	1.0	112	-4.3	11.0	-30.7	-2.3	13.1
stationbeta[52]	1.0	117	-4.5	11.3	-31.7	-2.8	13.2
stationbeta[53]	1.0	115	-4.5	11.3	-31.5	-3.0	12.9
stationbeta[54]	1.0	110	-4.4	11.1	-30.8	-2.5	13.2
stationbeta[55]	1.0	112	-4.4	11.2	-31.1	-2.4	13.0
stationbeta[56]	1.0	116	-4.7	11.3	-31.3	-2.7	13.3
stationbeta[57]	1.0	319	0.7	10.1	-16.9	0.2	25.1
stationbeta[58]	1.0	281	0.3	10.0	-17.5	-0.1	22.7
stationbeta[59]	1.0	304	0.2	10.1	-17.9	-0.0	23.9
stationbeta[60]	1.0	292	0.5	9.8	-16.1	-0.2	23.3
stationbeta[61]	1.0	333	1.0	9.8	-16.0	0.3	23.7
regionbeta[1]	1.0	146	-2.9	8.3	-23.1	-1.7	10.3
regionbeta[2]	1.0	194	-0.8	8.7	-18.1	-0.7	16.9
regionbeta[3]	1.0	185	-2.6	8.9	-23.9	-1.8	13.3
regionbeta[4]	1.0	226	0.4	9.2	-14.7	-0.4	22.2
regionbeta[5]	1.0	89	-4.4	9.7	-30.2	-2.4	9.0
regionbeta[6]	1.0	207	0.3	8.4	-14.3	-0.2	21.1

Table A.2: Diagnostics for the Bayesian Level 2 Model for Average Temperature.